УДК 539.12.01

QED EFFECTS OF HIGHER ORDERS IN DIS

*I. Akushevich**

North Carolina Cent. Univ., Durham, NC 27707 and TJNAF, Newport News, VA 23606, USA

E. Kuraev, B. Shaikhatdenov

Joint Institute for Nuclear Research, Dubna

*On leave from the National Centre of Particle and High Energy Physics, 220040 Minsk, Belarus.

УДК 539.12.01

QED EFFECTS OF HIGHER ORDERS IN DIS
*I. Akushevich**

North Carolina Cent. Univ., Durham, NC 27707 and TJNAF, Newport News, VA 23606, USA

E. Kuraev, B. Shaikhatdenov

Joint Institute for Nuclear Research, Dubna

The present status of theoretical description of deep inelastic scattering of leptons on protons with the account of radiative corrections (RC) in the leading and next-to-leading approximations is reviewed. For the process $ep \rightarrow ep\gamma$ along with RC coming from emission of virtual, soft and additional hard photons, there has been considered a e^+e^--pair production in the leading approximation. The Compton tensor with a heavy photon in the case of longitudinally polarized electron is presented. A cross section for a special experimental set-up with the tagging of additional hard photon is given to the nonleading order. A similar consideration is carried out for a cross channel, namely, electron–positron annihilation into hadrons with emission of a hard photon by initial leptons. Details of calculations are given in Appendices.

Дан обзор современного состояния теоретического описания процессов глубоконеупругого рассеяния лептонов на протонах с учетом радиационных поправок (РП) в лидирующем и следующем за лидирующим приближениях. Для процесса $ep \rightarrow ep\gamma$ наряду с РП от излучения виртуального, мягкого и жесткого дополнительного фотона в ведущем приближении также рассмотрено образование дополнительной e^+e^--пары. Приведен комптоновский тензор с тяжелым фотоном для случая продольно-поляризованного электрона. Для постановки опыта с детектированием дополнительного жесткого фотона представлено сечение с учетом нелидирующих поправок. Аналогичные результаты даны для кросс-канала — e^+e^--аннигиляции в адроны с излучением жесткого фотона начальными лептонами. В приложениях приводятся детали вычислений.

1. DEEP INELASTIC SCATTERING

Deep inelastic scattering (DIS) is one of the powerful tools in investigating a nucleon nature. It has played a key role to form our modern understanding of the substructure of hadrons. A number of experiments were performed at CERN, DESY, SLAC and elsewhere since the discovery of the proton structure in the late sixties. These experiments have provided very precise data in a wide kinematical region [1]. Renewed interest to the DIS was revived after measurement of the proton spin structure by EMC [2] (see also the review [3]). Till now the inclusive, semiinclusive and exclusive processes with both polarized

---

*On leave from the National Centre of Particle and High Energy Physics, 220040 Minsk, Belarus.

and unpolarized particles are widely investigated in many laboratories around the world.

Last years measurements of the observable quantities in DIS have the tendency to decrease both statistical and systematical errors comparing with the previous ones. Since radiative effects can give a substantial contribution to measured quantities the modern level of data analysis in experiments on DIS requires careful consideration of the QED radiative effects which can give substantial contribution to measured quantities. Usually a hard radiated photon cannot be registered in a detector. As is well understood the corrections due to soft photons and loop effects cannot be separated from observables in principle. Hence their contribution has to be calculated theoretically and subtracted from observed data. That's a reason why the calculation of radiative corrections is a very important field of theoretical particle physics.

Depending on the four-momentum transfer squared, Q^2, and the energy transfer, ν, there are three basic channels for lepton scattering on nuclei: elastic, quasielastic, and inelastic processes. In the case of elastic scattering ($\nu = Q^2/2M_A$, where M_A is a nuclear mass) leptons are scattered on a nucleus leaving the latter in its ground state. Quasielastic scattering ($\nu \sim Q^2/2M$, where M is a nucleon mass) corresponds roughly to direct collisions with the individual nucleons inside the nuclei. Inelastic scattering starts to appear when the pion threshold is reached ($\nu \geq Q^2/2M + m_\pi$, where m_π is a pion mass). At the Born level both Q^2 and ν are fixed completely by measuring the scattering angle and the energy (momentum) of scattered lepton. However at the level of radiative corrections, in the case of presence of real radiated photons, fixation is removed and the four-momentum of radiated photon has to be included in a kinematical variable calculation. Such elastic, quasielastic and inelastic processes with radiation of a real photon are known as radiative tails from the elastic ($\sigma_{\rm el}$) and the quasielastic ($\sigma_{\rm q}$) peaks and from the continuous spectrum ($\sigma_{\rm in}$) hereafter called shortly elastic, quasielastic and inelastic radiative tail.

The total radiative correction at the lowest order is obtained as a sum of these contributions together with loop corrections (σ_v) coming from effects of vacuum polarization and exchange by an additional virtual photon,

$$\sigma^{\rm rad.corr} = \sigma_{\rm in} + \sigma_{\rm q} + \sigma_{\rm el} + \sigma_v. \tag{1}$$

The lowest order radiative corrections in DIS on unpolarized proton target were first calculated by Mo and Tsai [4]. In this paper the integration region over the real photon phase space is divided into two parts by introducing an infinitesimal parameter. For values less than this parameter the integrals can be calculated analytically after some additional assumptions (arguments of structure functions are independent of photon momentum, only the leading power of photon energy is kept). The dependence on this unphysical infinitesimal parameter is a

shortcoming of this approach. A covariant formalism was developed in [5] in order to avoid the difficulties mentioned. The formulae of the lowest order RC are free of any approximation and rather compact, but are not visible as much as in the first approach. One of the shortcomings is the nonpositively defined expressions for inelastic radiative tail that make it unusable for Monte Carlo simulation of radiative processes. The excellent review of the model independent lowest order RC within this method can be found in [6]. Both approaches are widely used in practice. There are papers in which they were compared numerically [7, 8] and even analytically [9].

A complete set of the results for RC on unpolarized targets was obtained in [10]. The method was developed for the case of polarized proton and nuclear targets in [11,12]. QED correction to DIS cross section in the leading approximation was calculated in [13]. A lot of papers were devoted to electroweak radiative effects. We draw ones attention to the papers [14–17] in which the correction was calculated within a framework of electroweak theory basically for HERA kinematics. All cited papers were devoted to inclusive DIS. RC in the processes of semiinclusive and exclusive DIS electroproduction cannot be reduced to the inclusive case due to additional tensorial structures entering hadronic tensor and different phase space possible for hard radiated photon. Explicit results for these processes are given in papers [18–21]. Also we note papers [22–24] for RC to elastic and quasielastic ep scattering.

There is one more important task for theoreticians dealing with RC, namely a creation of computer tool which provides the procedure of accounting for RC to experimental data. One of the first codes applied in experiments on DIS at CERN were FERRAD [25] and TERAD [10] which were constructed on the basis of results of two discussed approaches, respectively. An exhaustive review of different codes can be found in [26]. We note recently developed codes gathering the best features and many years experience of data analysis. The Monte Carlo generator HERACLES [27] and semianalytical code HECTOR [28] are used in experiments at HERA. The code POLRAD 2.0 [29] and Monte Carlo generator RADGEN [9] are currently used in polarization experiments at CERN, DESY, SLAC and JLAB. For semiinclusive and exclusive cases the codes DIFFRAD [19] and HAPRAD [21] are intensively exploited. We note also the paper [30] where the approach to estimate a systematical error due to RC in polarized DIS is given.

Thus, we can conclude that the radiative correction of the lowest order is a well defined quantity. The open points here are basically related with a model dependent correction like a contribution of box diagrams or with generations to multiparticle measurements.

The next important step both from theoretical and experimental points of view is to take into account the second order radiative correction. So far, there are only approximate results even for model independent RC. Quite often results obtained by different authors are in disagreement and the quality of the approximations

made is not analyzed. The main approach here is the leading log approximation or put another way — the method of structure functions [31, 32]. Explicit results for inclusive higher order radiative correction within this approach were obtained in [13]. Correction to such a quite general quantity as the Compton tensor with heavy photon was discussed in [33]. If not to count a simple exponentiation formula, the higher order effects are not included in the procedure of RC accounting to experimental data. It is in the contradiction with currently performed experiments on Bhabha and $e\bar{e}$ annihilation where deeply analyzed second order correction is embedded into the standard scheme of data analysis.

The present review is just devoted to the consideration of different aspects of a theory of higher order effects in DIS. As such, it has something to do with the description of various sources of quantum corrections to the process. This way a very important second order contribution comes from elastic and quasielastic radiative tail. The kinematics is not trivial here and requires a careful consideration. These points and explicit results are discussed in Sec. 1.1. Very interesting measurements that allow one to obtain results for kinematical regions unreachable in normal DIS are experiments with photon tagging. RC come from higher order effects and are discussed in Sec. 1.2. Polarization effects for radiative processes can be considered in a quite general way by calculating the so-called Compton tensor for a heavy fermion. These results generalizing the ones obtained in [33] for unpolarized case are discussed in Sec. 1.3. And in Sec. 1.4, the hadronic cross section in $e\bar{e}$ annihilation with tagged photon is given.

1.1. QED Correction to Radiative Tail from Elastic Peak in DIS. Numerical analysis of the elastic radiative tail shows that its contribution is very important and can exceed the main measured process at the Born level. Therefore the next step is to calculate QED correction to the elastic radiative tail with the maximal possible accuracy. So far only the leading correction to elastic radiative tail due to double bremsstrahlung, which is part of the total second order correction, was treated numerically [16, 29] and the attempt to calculate the correction exactly was done in [34].

The structure of the cross section of elastic radiative tail is the following

$$\sigma^{\text{ERT}} \sim \int\limits_{Q^2_{h\ \text{min}}} \mathrm{d}Q_h^2 \mathcal{K}(Q_h^2, Q^2, W^2)\mathcal{F}^2(Q_h^2), \qquad (1.1.1)$$

where Q_h^2 is a momentum square transferred to hadronic system, and Q^2 and W^2 are leptonic kinematical variables measured. The quantity $\mathcal{K}$ is a kinematical factor known exactly and $\mathcal{F}$ is a nuclear form factor. Due to rapid fall of the form factor squared as a function of Q_h^2 the main integration region is close to the lower integration limit. In papers [16, 35] this fact was used to construct an approximation, where Q_h^2 is considered as a small parameter of order of the proton mass squared. In this paper we will also use this approximation to analyze

the correction to elastic radiative tail. The application of Sudakov technique will allow us to obtain compact explicit formulae for processes considered. The first effect which has to be considered is the one-loop correction and the emission of additional real photon. We will analyze both of them at leading and next-to-leading levels. Another effect contributing to the cross section is a lepton pair creation. We will calculate it in the leading log approximation.

Obtaining a second order correction to deep inelastic scattering is the main motivation of this part. However our results can be used in other cases. For instance, they can be considered as a radiative correction in measurements with hard photon detected in coincidence with scattered lepton (see [36], for example), that allows one to reach kinematical regions otherwise unreachable. That is why we do not concretize our notation usually used in DIS but instead try to keep it as general as possible. In the next section we introduce our notation and obtain results for the cross section of single bremsstrahlung using Sudakov technique. In Section 1.1.2. we give results for one-loop corrections. Double bremsstrahlung and contributions due to pair production are considered in Sections 1.1.3. and 1.1.4. and final remarks are given in Section 1.1.5. Some technical details are discussed in Appendices.

1.1.1. Single Bremsstrahlung. We study the process

$$
\begin{aligned}
&e(p_1) + p(p_2) \rightarrow e(p_1') + \gamma(k_1) + p(p_2'), \quad s = 2p_1 p_2, \\
&Q_h^2 = -(p_2 - p_2')^2, \quad Q^2 = 2p_1 p_1', \quad k_1^2 = 0, \\
&p_1^2 = p_1'^2 = m^2, \quad p_2^2 = p_2'^2 = M^2, \quad q^2 = -O_h^2,
\end{aligned}
\tag{1.1.2}
$$

in the kinematical region

$$
s \gg Q^2 > Q_h^2 \sim M^2, \qquad 2p_2 p_1' \sim s. \tag{1.1.3}
$$

The expression for differential cross section in Born approximation looks (details are given in Appendix A):

$$
2\varepsilon_1' \frac{\mathrm{d}^3 \sigma_0^\gamma}{\mathrm{d}^3 p_1'} = \frac{4\alpha^3}{\pi^2} \int \frac{\mathrm{d}^2 \mathbf{q}}{(\mathbf{q}^2 + Q_{\min}^2)^2} \frac{1}{1-b} \Phi^\gamma \Phi^{\mathrm{prot}}, \tag{1.1.4}
$$

with $b = 2p_2 p_1'/s$ the energy fraction of the scattered electron. We imply the Sudakov parameterization of the 4-momenta in the problem (see Appendix A).

Note that due to the gauge invariance condition

$$
q^\rho J_\rho^{(1)} \approx (\alpha_q p_2 + q_\perp)^\rho J_\rho^{(1)} = 0, \tag{1.1.5}
$$

the quantity Φ^γ is constructed out of $(1/s)p_2 J^{(1)}$ which may be rearranged as follows:

$$
\begin{aligned}
\frac{1}{s} p_2^\mu J_\mu^{(1)} &= -\frac{s}{s_1} |\mathbf{q}| e_q^\mu J_\mu^{(1)}, \quad e_q = \frac{\mathbf{q}}{|\mathbf{q}|}, \\
s_1 &= s\alpha_q = (p_1' + k_1)^2 + \mathbf{q}^2 - m^2.
\end{aligned}
\tag{1.1.6}
$$

Thus Φ^γ vanishes for small $\mathbf{q}^2$. The explicit expression for Φ^{prot} is found to be

$$\Phi^{\mathrm{prot}} = 2(F_1^2 + \frac{\mathbf{q}^2}{M^2} F_2^2). \tag{1.1.7}$$

For Φ^γ we have (we refer for further details to Appendix A):

$$\Phi^\gamma = \frac{(1-b)^2 b(1+b^2)\mathbf{q}^2}{n_1 n}, \tag{1.1.8}$$

with

$$n = (\mathbf{p}_1' - b\mathbf{q})^2, \quad n_1 = (\mathbf{p}_1' - \mathbf{q})^2. \tag{1.1.9}$$

Another fact is that both $\Phi^\gamma/\mathbf{q}^2$ and Φ^{prot} do not vanish in the limit of small momentum transfer $|\mathbf{q}|$, thus providing the logarithmic enhancement upon performing the $Q_h^2 \approx \mathbf{q}^2$ integration (Weizsäcker–Williams approximation). Indeed, the quantity $Q_{\min}^2$ entering the cross section is a small quantity,

$$Q_{\min}^2 = M^2 \left(\frac{Q^2}{(1-b)s} \right)^2 \ll M^2. \tag{1.1.10}$$

For completeness we put the phase volume of the scattered electron in terms of Sudakov variables:

$$\frac{\mathrm{d}^3 p_1'}{2\varepsilon_1'} = \frac{\mathrm{d}b}{2b} \mathrm{d}^2 \mathbf{p}_1', \quad Q^2 = 2p_1 p_1' = \frac{\mathbf{p}_1'^2}{b}. \tag{1.1.11}$$

Note that the requirement $Q^2 > Q_h^2$ provides the absence of singularities while doing an integration over $\mathrm{d}^2\mathbf{q}$.

1.1.2. Virtual and Soft Photon Emission Contribution. The correction coming from the emission of virtual and soft photons (in the cms reference frame) can be drawn out of paper [33], in which the radiative corrections to the Compton tensor were calculated

$$2\varepsilon_1' \frac{\mathrm{d}^3 \sigma_{B+V+S}}{\mathrm{d}^3 p_1'} = 2\varepsilon_1' \frac{\mathrm{d}^3 \sigma_0^\gamma}{\mathrm{d}^3 p_1'} \left[1 + \frac{\alpha}{2\pi} \tilde{\rho} + \right.$$
$$\left. + \frac{\alpha}{4\pi} \frac{1}{1+b^2} \left(\tau_{11} + b(\tau_{12} + \tilde{\tau}_{12}) + b^2 \tilde{\tau}_{11} \right) \right], \tag{1.1.12}$$

with

$$\tilde{\rho} = 2(L-1)(2\ln\Delta - \ln b) + 3L_h - \ln^2 b -$$
$$- \frac{9}{2} - \frac{\pi^2}{3} + 2\mathrm{Li}_2\left(\cos^2\frac{\theta}{2}\right), \qquad (1.1.13)$$
$$L = \ln\frac{Q^2}{m^2}, \qquad L_h = \ln\frac{Q_h^2}{m^2},$$
$$\Delta = \frac{\Delta E}{E}, \qquad \mathrm{Li}_2(x) = -\int\limits_0^x \frac{\ln(1-y)}{y}\mathrm{d}y.$$

The Born cross section after substitution of Eq. (1.1.8) into Eq. (1.1.4) and neglect of subleading terms becomes

$$2\varepsilon_1' \frac{\mathrm{d}^3\sigma_0^\gamma}{\mathrm{d}^3 p_1'} = \frac{4\alpha^3}{\pi^2}\int \frac{\mathrm{d}^2\mathbf{q}\mathbf{q}^2}{(\mathbf{q}^2 + Q_{\min}^2)^2}\frac{(1-b)(1+b^2)}{b(Q^2)^2}\Phi^{\mathrm{prot}},$$

where $\Delta E, E$ are the upper bound on the undetectable soft photon energy, and the energy of the initial electron, respectively; θ is the angle in the laboratory reference frame between the initial and the scattered electron momenta. Somewhat cumbersome functions τ_{ij} are explicitly given in Appendix D. It should be noted that they do not contain any large logarithms but include the quantity Q_h^2 which is small in our approximation. If one keeps only nonzero terms in the expansion over Q_h^2, then

$$\frac{1}{2}\left(\tau_{11} + b(\tau_{12} + \tilde{\tau}_{12}) + b^2\tilde{\tau}_{11}\right) = \left[3\log\frac{Q^2}{Q_h^2(1-b)} - 1\right]\times$$
$$\times(1+b^2) + 4b\log(1-b) + [b^2 + (1-b)^2]\times$$
$$\times\left[\log^2\frac{(1-b)}{b} + \pi^2\right] + [1 + (1-b)^2]\log^2(1-b) +$$
$$+(3-2b)\log b. \qquad (1.1.14)$$

The logarithms $\log Q_h^2$ cancel out exactly in the sum of (1.1.14) and $\tilde{\rho}$.

1.1.3. Two Hard Photons Emission Contribution. We will consider now the process of two hard photons emission:

$$e(p_1) + p(p_2) \to e(p_1') + \gamma(k_1) + \gamma(k_2) + p(p_2'). \qquad (1.1.15)$$

The relevant contribution to the cross section looks

$$2\varepsilon_1' \frac{\mathrm{d}^3\sigma}{\mathrm{d}^3 p_1'} = \frac{\alpha^4}{8\pi^4}\int \frac{\mathrm{d}^2\mathbf{q}}{(\mathbf{q}^2 + Q_{\min}^2)^2}\frac{\mathrm{d}x_1\mathrm{d}^2\mathbf{k}_1}{x_1 x_2}\Phi^{\gamma\gamma}\Phi^{\mathrm{prot}},$$
$$Q_{\min}^2 = M^2\left(\frac{s_1}{s}\right)^2, \quad s_1 = (p_1' + k_1 + k_2)^2, \qquad (1.1.16)$$

with the expression for Φ^{prot} given earlier. The explicit form of $\Phi^{\gamma\gamma}$ can be found in Appendix B. The integration over $\mathrm{d}^2\mathbf{k}_1$ may be performed using the integrals given in Appendix C.

Concerning the region $Q_h^2 \ll Q^2$, the result is found to be [*]

$$
\begin{aligned}
\Phi^{\gamma\gamma} &= 16\mathbf{q}^2 \left\{ \frac{Q^2}{s_1^2} \left[\frac{s_1^2(1+b^2)}{d_1 d_2 d_1' d_2'} + \frac{d_1^2 + d_1'^2}{b s_1^2 d_2 d_2'} + \frac{d_2^2 + d_2'^2}{b s_1^2 d_1 d_1'} \right] - \right. \\
&\quad - \frac{2}{Q^4}(1 + \mathcal{P}_{12}) \left[\frac{m^2}{d_1^2} \frac{x_2^2(b^2 + (1-x_1)^2)}{b(1-x_1)^3} + \right. \\
&\quad \left. \left. + \frac{m^2}{d_1'^2} \frac{x_2^2 b^2 (1 + (1-x_2)^2)}{(1-x_2)^3} \right] \right\}
\end{aligned}
\tag{1.1.17}
$$

with the notations introduced

$$
s_1 = \frac{\mathbf{k}_1^2}{x_1} + \frac{\mathbf{k}_2^2}{x_2} + \frac{\mathbf{p}_1'^2}{b}, \qquad d_i = \frac{1}{x_i}(m^2 x_i^2 + \mathbf{k}_i^2),
\tag{1.1.18}
$$

$$
d_i' = \frac{1}{x_i b}[m^2 x_i^2 + (x_i \mathbf{p}_1' - b\mathbf{k}_i)^2],
$$

where $x_{1,2}$ are the energy fractions of hard photons, $x_1 + x_2 + b = 1$. Besides we use the relations

$$
\mathbf{k}_1 + \mathbf{k}_2 + \mathbf{p}_1' = 0, \quad 2q p_1' = s_1 b, \quad s_1 = 2q p_1 = s\alpha_q.
$$

An integration over $\mathrm{d}^2\mathbf{k}_1$ may be performed analytically and to a logarithmic accuracy it boils down to

$$
\int \frac{\mathrm{d}^2\mathbf{k}_1}{\pi} \left[\frac{1}{d_1}; \frac{1}{d_2}; \frac{1}{d_1'}; \frac{1}{d_2'} \right] = L\left[x_1; x_2; \frac{x_1}{b}; \frac{x_2}{b} \right].
\tag{1.1.19}
$$

The resulting contribution (again to a logarithmic accuracy) takes the following form

$$
\begin{aligned}
\int \mathrm{d}^2\mathbf{k}_1 \Phi^{\gamma\gamma} &= \frac{16\pi\mathbf{q}^2 L}{b(Q^2)^2}(1 + \mathcal{P}_{12}) x_2^2 \times \\
&\quad \times \left[\left(1 + \frac{1}{(1-x_1)^2} + \frac{b^2}{(1-x_2)^2} \right)(1 + b^2) + \right. \\
&\quad \left. + \frac{b^2}{(1-x_1)^4} + \frac{b^4}{(1-x_2)^4} \right], \\
\Delta &< x_i < 1 - b - \Delta.
\end{aligned}
\tag{1.1.20}
$$

---

[*]Upon applying the crossing transformation to the amplitude of $e\bar{e}$ annihilation to $\gamma\gamma\gamma$ presented in paper [37].

Carrying out the integration of Eq. (1.1.17) over $\mathbf{k}_1$ and x_1 to a next-to-leading accuracy we obtain for the contribution to the differential cross section coming from emission of two hard photons

$$2\varepsilon_1' \frac{\mathrm{d}^3\sigma^{\gamma\gamma}}{\mathrm{d}^3 p_1'} = \frac{2\alpha^4}{\pi^3} \int \frac{\mathrm{d}^2\mathbf{q}}{(\mathbf{q}^2 + Q_{\min}^2)^2} \frac{\mathbf{q}^2(T_{LL} + T_{NLO})}{b(Q^2)^2} \Phi^{\mathrm{prot}}, \qquad (1.1.21)$$

where the leading and next-to-leading contributions read

$$
\begin{aligned}
T_{LL} &= (L-1)[4(1-b)(1+b^2)\ln\frac{1-b}{\Delta} + \\
&+ (1-b)(1-b^2)\ln b - \frac{2}{3}(1-b)(7-2b+7b^2)], \\
T_{NLO} &= -\frac{1}{2}\frac{b^4+6b^2+1}{1+b}\log^2 b - \\
&- \frac{1}{3}(3-b^2)(3-b)\log b + \\
&+ \frac{8}{3}(1-b)(b^2+b+1)\log(1-b) - \\
&- (1-b)\Big[\frac{1}{3}(15b^2-2b+15) + \\
&+ 2\Big(\mathrm{Li}_2(b) - \frac{\pi^2}{6}\Big)\frac{b^4+6b^2+1}{1-b^2}\Big].
\end{aligned}
$$

$$(1.1.22)$$

There are two possible experimental set-ups we concern with: the first one in which a recoil proton is registered, and the second — pure inclusive set-up — with only a final lepton observed. Definitely, NLO contribution obtained can be counted valid only for the former experimental set-up, while in the latter case one can use the expression given above only to an LL accuracy.

The general answer for the cross section in Born approximation with the lowest order correction to the leading approximation is a sum of the contributions coming from virtual and real soft photons emission given above as well as from two hard photons emission and is free from dependence on the auxiliary parameter Δ.

The graphs given below illustrate behavior featured by the complete QED RC contribution to the cross section of DIS as well as the comparative contributions of the LL, NLO terms and of the correction due to pair production.

1.1.4. Contribution of Lepton Pair Production. Consider now the hard pair production process that takes place at the same order of perturbation theory as the two hard photons emission. In the same way we may conclude that the soft pair case as well as the case of double collinear kinematics does not contribute

to the radiative tail. Therefore we may consider only semicollinear kinematics of hard pair production of which there exist two different mechanisms [38]. One of these is the two-photon mechanism of pair creation. An electron from that pair having momentum p_1' is detected in experiment and the scattered electron moves close to the initial electron direction. This kinematics permits us to apply the Weizsäcker–Williams approximation,

$$2\varepsilon_1' \frac{\mathrm{d}^3\sigma_{\mathrm{pair}}^{(1)}}{\mathrm{d}^3 p_1'} \;\;=\;\; \frac{2\alpha^4}{\pi^3} \int \frac{\mathrm{d}^2\mathbf{q}}{(\mathbf{q}^2 + Q_{\min}^2)^2} \frac{\mathbf{q}^2 L}{b(Q^2)^2} \Phi^{\mathrm{prot}} \times$$

$$\times \;\; \frac{\mathrm{d}\beta_-}{(1 - \beta_-)^4}((1 - \beta_- - b)^2 + b^2)(1 + \beta_-^2), \quad (1.1.23)$$

$$s_1 \;\;=\;\; Q^2 \frac{1 - \beta_-}{\beta_+}, \qquad b + \beta_- + \beta_+ = 1.$$

The second mechanism is characterized by the bremsstrahlung mechanism of pair creation, with an electron from a pair to be detected. Leaving details to Appendix E let us present here the result

$$2\varepsilon_1' \frac{\mathrm{d}^3\sigma_{\mathrm{pair}}^{(2)}}{\mathrm{d}^3 p_1'} \;\;=\;\; \frac{2\alpha^4}{\pi^3} \int \frac{\mathrm{d}^2\mathbf{q}}{(\mathbf{q}^2 + Q_{\min}^2)^2} \frac{\mathbf{q}^2 L}{(Q^2)^2} \Phi^{\mathrm{prot}} \times$$

$$\times \;\; \frac{b(1 + \beta_-^2)\mathrm{d}\beta_-}{(1 - \beta_-)^4}[(1 - b - \beta_-)^2 + b^2], \qquad (1.1.24)$$

$$s_1 \;\;=\;\; Q^2 \frac{1 - \beta_-}{b\beta_-}.$$

The integration over β_- can be performed analytically with additional assumption that $Q_{\min}^2$ has no β_- dependence. The result for the sum of these contributions is found to be

$$2\varepsilon_1' \frac{\mathrm{d}^3\sigma_{\mathrm{pair}}}{\mathrm{d}^3 p_1'} \;\;=\;\; \frac{2\alpha^4}{\pi^3} \int \frac{\mathrm{d}^2\mathbf{q}}{(\mathbf{q}^2 + Q_{\min}^2)^2} \frac{\mathbf{q}^2 L(1 + b^2)}{b(Q^2)^2} \Phi^{\mathrm{prot}} \times$$

$$\times \;\; \left(1 - b + 2(1 + b)\log b + \frac{4}{3b}(1 - b^3)\right). \qquad (1.1.25)$$

1.1.5. Discussion. In this part the correction to radiative tail from elastic peak is studied in the kinematics when a final lepton is measured. Using Sudakov technique the contributions of loops (1.1.12), double photon bremsstrahlung (1.1.21) and a pair production (1.1.23,1.1.24) are calculated.

In this section we analyze obtained contributions numerically. Both the relative contributions of the processes considered and the total correction to the lowest order process are investigated within kinematical conditions of experiments on electron DIS at TJNAF and DESY (both for HERA and for HERMES). It is convenient to define the following quantities:

$$\delta = \frac{\sigma_L + \sigma_N + \sigma_p}{\sigma_0}, \quad \delta_{L,N,p} = \frac{\sigma_{L,N,p}}{\sigma_0}. \tag{1.1.26}$$

Here σ_0 stands for the cross section of radiative tail from elastic peak (1.1.4). Other σ's constitute the next order results. The quantity σ_p is a direct sum of two mechanisms of pair creations (1.1.23,1.1.24), whereas σ_L and σ_N are the leading (including mass singularities terms $\log(Q^2/m^2)$) and next-to-leading (independent of leptonic mass) terms. They are obtained upon summing up expressions given in Eqs. (1.1.12) and (1.1.21) after cancellation of infrared divergence.

The relative radiative correction to elastic radiative tail is important practically everywhere. The modern level of data analysis and very high experimental accuracies achieved in current experiments on DIS require that a generalization of standard radiative correction procedure be made in order to include a second order radiative correction. An extremely interesting region where the correction considered is important is actually high y domain. Remind, that this one (up to $y \sim 0.95$) is under investigation at TJNAF.

The main contribution to a second-order radiative correction comes from the effect of pair creation. Asymptotical behavior of σ_p for small $b = 1 - y$ is $1/b^2$ whereas the other cross sections feature only $1/b$ behavior. That is in fact a reason of the large correction in the region of high y. In the paper presented this particular contribution is calculated in the leading approximation only, therefore a study of the correction, induced by a pair production, at the next-to-leading level is highly desirable.

The relative contribution of the next-to-leading correction σ_N is not small with respect to the leading log contribution σ_L. In the region of large y the relative contribution σ_N/σ_L does not exceed 5%, whereas for small y it can reach as much as 20–30%. From the other hand the next-to-leading contribution completely fixes all uncertainties of leading log approximation thus leaving unknown only terms proportional to lepton mass squared and Q_h^2, which is effectively small due to behavior of form factors.

1.2. Tagged Photon with Next-to-Leading Accuracy. The radiative corrections to deep inelastic electron proton scattering due to hard real photon emission are very important in certain regions of the HERA kinematic domain. In fact, the initial-state collinear radiation leads to a reduction of the projectile electron energy and therefore to a shift of the effective Bjorken variables in the hard scattering process as compared to those determined from the actual measurement

of the scattered electron alone. Therefore, radiative events

$$e(p_1) + p(P) \rightarrow e(p_2) + \gamma(k) + X + (\gamma), \qquad (1.2.1)$$

are to be carefully taken into account [4, 6, 39].

On the other hand, measuring the energy of the photons emitted very close to the incident electron beam direction [40–43] permits one to overlap the kinematical region of photoproduction ($Q^2 \approx 0$) and the DIS region with small transferred momenta (about a few GeV^2) within the high energy HERA experiments. Furthermore, these radiative events may be used to independently determine the proton structure functions F_2 and F_1 (and therefore F_L) in a single run without lowering the beam energies [36, 41]. Preliminary results of an F_2 analysis using such radiative events were recently presented by the H1 collaboration [44].

Our aim is to calculate the radiative corrections to neutral current deep inelastic events with simultaneous (exclusive) detection of a hard photon emitted very close to the direction of the incoming electron beam ($\theta_\gamma = \widehat{\mathbf{p}_1 \mathbf{k}} \leq \theta_0 \approx \approx 5 \cdot 10^{-4}$ rad). In the case of the HERA collider, the experimental detection of photons emitted in this very forward direction is actually possible due to the presence of photon detectors (PD) that are part of the luminosity monitoring system of ZEUS and H1.

Let us briefly review the kinematics for the process under consideration. As the opening angle of the forward photon detector is very small, and since we will only consider cross sections where the tagged photon is integrated over the solid angle covered by this photon detector, we can parameterize these radiative events using the standard Bjorken variables x and y, that are determined from the measurement of the scattered electron,

$$x = \frac{Q^2}{2P \cdot (p_1 - p_2)}, \quad y = \frac{2P \cdot (p_1 - p_2)}{V}, \quad Q^2 = 2p_1 \cdot p_2 = xyV, \quad (1.2.2)$$

with $V = 2P \cdot p_1$, and the energy fraction z of the electron after initial state radiation of a collinear photon,

$$z = \frac{2P \cdot (p_1 - k)}{V} = \frac{\varepsilon - k^0}{\varepsilon}, \qquad (1.2.3)$$

where ε is the initial electron energy, and k^0 is the energy seen in the forward photon detector.

An alternative set of kinematic variables that is especially adapted to the case of collinear radiation, is given by the *shifted* Bjorken variables [41],

$$\hat{Q}^2 = -(p_1 - p_2 - k)^2, \quad \hat{x} = \frac{\hat{Q}^2}{2P \cdot (p_1 - p_2 - k)}, \quad \hat{y} = \frac{P \cdot (p_1 - p_2 - k)}{P \cdot (p_1 - k)}.$$
$$(1.2.4)$$

The relations between the shifted and the standard Bjorken variables read [41]:

$$\hat{Q}^2 = zQ^2, \qquad \hat{x} = \frac{xyz}{z+y-1}, \qquad \hat{y} = \frac{z+y-1}{z}. \qquad (1.2.5)$$

The cross section under consideration in the Born approximation, integrated over the solid angle of the photon detector ($0 \le \theta_\gamma \le \theta_0$, $\theta_0 \ll 1$), then takes the following form:

$$\frac{z}{y} \frac{\mathrm{d}^3 \sigma_{\mathrm{Born}}}{\mathrm{d}x\,\mathrm{d}y\,\mathrm{d}z} = \frac{1}{\hat{y}} \frac{\mathrm{d}^3 \sigma_{\mathrm{Born}}}{\mathrm{d}\hat{x}\,\mathrm{d}\hat{y}\,\mathrm{d}z} = \frac{\alpha}{2\pi} P(z, L_0) \tilde{\Sigma}, \qquad (1.2.6)$$

where

$$\tilde{\Sigma} = \Sigma(\hat{x}, \hat{y}, \hat{Q}^2) \;\; = \;\; \frac{2\pi\alpha^2(-\hat{Q}^2)}{\hat{Q}^2 \hat{x}\hat{y}^2} F_2(\hat{x}, \hat{Q}^2) \Big[2(1-\hat{y}) - 2\hat{x}^2\hat{y}^2 \frac{M^2}{\hat{Q}^2} +$$

$$+ \;\; \Big(1 + 4\hat{x}^2 \frac{M^2}{\hat{Q}^2}\Big) \frac{\hat{y}^2}{1+R} \Big],$$

$$P(z, L_0) = \frac{1+z^2}{1-z} L_0 - \frac{2z}{1-z}, \;\; R = R(\hat{x}, \hat{Q}^2) = \Big(1 + 4\hat{x}^2 \frac{M^2}{\hat{Q}^2}\Big) \frac{F_2(\hat{x}, \hat{Q}^2)}{2\hat{x} F_1(\hat{x}, \hat{Q}^2)} - 1,$$

$$\alpha(-\hat{Q}^2) = \frac{\alpha}{1 - \Pi(-\hat{Q}^2)}, \;\; L_0 = \ln\Big(\frac{\varepsilon^2 \theta_0^2}{m^2}\Big), \;\; \hat{Q}^2 = 2zp_1 \cdot p_2 = 2z\varepsilon^2 Y(1-c),$$

$$Y = \frac{\varepsilon_2}{\varepsilon} = 1 - y + xy \frac{E_p(1+\beta_p)}{2\varepsilon}, \;\; c = \cos(\widehat{\boldsymbol{p}_1 \boldsymbol{p}_2}),$$

$$\hat{x} = \frac{\hat{Q}^2}{2P \cdot (zp_1 - p_2)} = \frac{z\varepsilon Y(1-c)}{zE_p(1+\beta_p) - YE_p(1+\beta_p c)}, \;\; \beta_p = \sqrt{1 - M^2/E_p^2},$$

$$\hat{y} = \frac{2P \cdot (zp_1 - p_2)}{zV} = \frac{z(1+\beta_p) - Y(1+\beta_p c)}{z(1+\beta_p)}. \qquad (1.2.7)$$

The quantities F_2 and F_1 are the proton structure functions, M and m are the proton and electron masses, respectively. In the cross section (1.2.6) we take into account terms proportional to $M^2/\hat{Q}^2$, which may be important at low Q^2. Note that the neglect of Z-boson exchange and γ–Z interference is a good approximation, because we are interested mostly in events with small momentum transfer $\hat{Q}^2$.* The energies of the initial and final electron, of the tagged photon

---

*The corresponding Born cross section including contributions from the Z can be found in Ref. 42.

and of the initial proton (ε, ε_2, k^0, and E_p) are defined in the laboratory reference frame (i.e., the rest frame of HERA detectors). The cross section (1.2.6) agrees with [41, 42]. Also note that we explicitly included the correction from the vacuum polarization operator $\Pi(-\hat{Q}^2)$ in the virtual photon propagator. The aim of our work is to calculate the higher order QED radiative corrections for this process in the leading and next-to-leading logarithmic approximation.

Here we will restrict ourselves to the model independent QED radiative corrections related to the lepton line, which form a complete, gauge invariant subset for the neutral current scattering process. The remaining source of QED radiative corrections at the same order, such as virtual corrections with double photon exchange and bremsstrahlung off the partons are more involved and model dependent, they will be considered elsewhere. Our approach to the calculation of the QED corrections is based on the utilization of all essential Feynman diagrams that describe the observed cross section in the framework of the used approximation. The same approach was used recently for the calculation of the QED corrections for the small angle Bhabha scattering cross section at LEP1 [45].

This part is organized as follows. Section 1.2.1 is devoted to the corrections related with emission of virtual and soft real photons in the hard collinear photon emission DIS process. In Sec. 1.2.2 we consider the radiative corrections due to emission of two hard photons in the collinear kinematics (where we distinguish between the cases when both photons are emitted close to the initial electron direction and the case when one of the photons is emitted along the initial and the other one along the scattered electron direction) and the semicollinear kinematics, where the additional hard photon is emitted at a large angle. Section 1.2.3 collects the results obtained and discusses two experimental cases: an exclusive set-up, that assumes that a bare electron can be measured, and a calorimetric one. The Appendices are devoted to details of the calculation.

1.2.1. Virtual and Soft Photon Emission Corrections. In order to calculate the contributions from the virtual and soft photon emission corrections, we start from the expression for the Compton scattering tensor with a heavy photon [33, 46],

$$K_{\mu\nu} = (8\pi\alpha)^{-1} \sum_{\text{spins}} M_\mu^{e\gamma^* \to e'\gamma}(M_\nu^{e\gamma^* \to e'\gamma})^*, \qquad (1.2.8)$$

where M_μ is the matrix element of the process of Compton scattering

$$\gamma^*(-q) + e(p_1) \to \gamma(k) + e(p_2), \qquad (1.2.9)$$

and the index μ describes the polarization state of the virtual photon. This tensor is conveniently decomposed as follows:

$$K_{\mu\nu} = \frac{1}{2}(P_{\mu\nu} + P^*_{\nu\mu}), \tag{1.2.10}$$

$$P_{\mu\nu} = \tilde{g}_{\mu\nu}(B_g + \frac{\alpha}{2\pi}T_g) + \tilde{p}_{1\mu}\tilde{p}_{1\nu}(B_{11} + \frac{\alpha}{2\pi}T_{11}) +$$

$$+ \tilde{p}_{2\mu}\tilde{p}_{2\nu}(B_{22} + \frac{\alpha}{2\pi}T_{22}) + \frac{\alpha}{2\pi}(\tilde{p}_{1\mu}\tilde{p}_{2\nu}T_{12} + \tilde{p}_{2\mu}\tilde{p}_{1\nu}T_{21}),$$

$$\tilde{g}_{\mu\nu} = g_{\mu\nu} - \frac{q_\mu q_\nu}{q^2}, \qquad \tilde{p}_{1\mu} = p_{1\mu} - q_\mu\frac{p_1 \cdot q}{q^2},$$

$$\tilde{p}_{2\mu} = p_{2\mu} - q_\mu\frac{p_2 \cdot q}{q^2}, \qquad p_1 = q + p_2 + k.$$

The expressions for the quantities B_{ij} corresponding to the Born approximation are [*]:

$$B_g = \frac{1}{st}\left[(s+u)^2 + (t+u)^2\right] - 2m^2q^2\left(\frac{1}{s^2} + \frac{1}{t^2}\right), \quad B_{11} = \frac{4q^2}{st} - \frac{8m^2}{s^2},$$

$$B_{22} = \frac{4q^2}{st} - \frac{8m^2}{t^2}, \quad s = 2p_2 \cdot k, \quad t = -2p_1 \cdot k, \quad u = (p_2 - p_1)^2,$$

$$q^2 = s + t + u, \quad p_1^2 = p_2^2 = m^2, \quad k^2 = 0. \tag{1.2.11}$$

The one-loop QED corrections are contained in the quantities T_{ij}, whose explicit expressions are given in [33, 46]. Here we have to integrate them over the solid angle of the emitted photon corresponding to the shape of the photon detector. We need to keep only the terms singular in the limit $\theta_\gamma \to 0$, since after integration the constant terms contribute only proportional to $\theta_0^2 \sim 10^{-6}$ and can be safely neglected. Another simplification comes from the fact that we need only the symmetric (and real) part of the tensor K. This way, by using typical integrals

$$\int \frac{d\Omega_k}{2\pi}\frac{1}{t} = -\frac{L_0}{2\varepsilon^2(1-z)}, \qquad \int \frac{d\Omega_k}{2\pi}\frac{m^2}{t^2} = \frac{1}{2\varepsilon^2(1-z)^2}, \tag{1.2.12}$$

and using the expressions given in Appendix F we obtain the following expression for the Compton tensor integrated over the angular part of the photon phase space:

$$\int \frac{d\Omega_k}{2\pi}K_{\mu\nu} = \left(-Q_l^2 g_{\mu\nu} + 4zp_{1\mu}p_{1\nu}\right)\frac{1}{2\varepsilon^2(1-z)}\left[\left(1 + \frac{\alpha}{2\pi}\rho\right)P(z, L_0) - \frac{\alpha}{2\pi}T\right],$$

---

[*]We have already dropped those terms that vanish in the high-energy limit when one integrates over any finite region of photon phase space.

$$\rho = 4 \ln \frac{\lambda}{m}(L_Q - 1) - L_Q^2 + 3L_Q + 3 \ln z + \frac{\pi^2}{3} - \frac{9}{2}, \qquad (1.2.13)$$

$$T = \frac{1 + z^2}{1 - z}(A \ln z + B) - \frac{4z}{1 - z}L_Q \ln z - \frac{2 - (1 - z)^2}{2(1 - z)}L_0 + O(1),$$

$$A = -L_0^2 + 2L_0 L_Q - 2L_0 \ln(1 - z), \qquad B = \left(\ln^2 z - 2\mathrm{Li}_2(1 - z)\right)L_0,$$

$$L_Q = \ln \frac{Q^2}{m^2}, \qquad \mathrm{Li}_2(x) = -\int_0^x \frac{\mathrm{d}y}{y} \ln(1 - y).$$

The quantity λ, which enters into the expression for ρ, is a fictitious photon mass.

In the construction of the total expression for the tensor $K_{\mu\nu}$ we replaced $q_\mu = q_\nu = 0$, $p_{2\mu,\nu} = z p_{1\mu,\nu}$, bearing in mind the gauge invariance of hadronic tensor [47],

$$H_{\mu\nu} = \frac{4\pi}{M}\left(W_2(x_h, Q_h^2)\tilde{P}_\mu\tilde{P}_\nu - M^2 W_1(x_h, Q_h^2)\tilde{g}_{\mu\nu}\right), \qquad (1.2.14)$$

$$x_h = \frac{Q_h^2}{2P \cdot q_h}, \qquad \tilde{P}_\nu = P_\nu - q_{h\nu}\frac{P \cdot q_h}{q_h^2}.$$

Here we imply $q_h = q$, $Q_h^2 = -q^2$.

Consider now the process with emission of a soft photon in addition to the emission of the hard one, which hits the PD. We imply the condition that the energy of the soft photon should be less than some small quantity $\delta\varepsilon$ (in the centre-of-mass system). In straightforward calculations, starting from Feynman diagrams, some care is to be paid in the evaluation of integrals over the phase volume of the soft photon, as some contributions are crucially dependent on the correlation between our two small parameters $\Delta = \delta\varepsilon/\varepsilon$ and θ_0. In our particular case $\theta_0 \ll \Delta \ll 1$, the result coincides with the one obtained using the approximation of classical currents for soft photons. The total effect for the sum of contributions of virtual and soft photon emission consists in the replacement of the quantity ρ by $\tilde{\rho}$ in Eq. (1.2.13) (see Eq. (45) in [33, 46]):

$$\rho \to \tilde{\rho} = 2(L_Q - 1)\ln \frac{\Delta^2}{Y} + 3L_Q + 3 \ln z - \ln^2 Y - \frac{\pi^2}{3} - \qquad (1.2.15)$$
$$- \frac{9}{2} + 2\mathrm{Li}_2\left(\frac{1 + c}{2}\right).$$

The final expression for the virtual and soft photon emission corrected tagged photon cross section has the form

$$\frac{z}{y}\frac{\mathrm{d}^3\sigma_{VS}}{\mathrm{d}x\,\mathrm{d}y\,\mathrm{d}z} = \left(\frac{\alpha}{2\pi}\right)^2 [P(z, L_0)\tilde{\rho} - T]\tilde{\Sigma}. \qquad (1.2.16)$$

1.2.2. Double Hard Bremsstrahlung. Consider now the emission of an extra photon with the energy more than $\delta\varepsilon$. For the calculation of the contributions from real hard bremsstrahlung, which in our case correspond to double photon emission with at least one photon seen in the forward detector, we specify three specific kinematical domains: *i)* both hard photons strike the forward photon detector, i.e., both are emitted within a narrow cone around the electron beam ($\theta \leq \theta_0$); *ii)* one hard photon is tagged by the PD, while the other is collinear to the outgoing electron ($\theta_2 = \widehat{\mathbf{k}_2 \mathbf{p}_2} \leq \theta_0'$); and finally *iii)* the second photon is emitted at large angles (i.e., outside the defined narrow cones) with respect to both incoming and outgoing electron momenta. We denominate the third kinematical domain as a semicollinear one. The contributions of the regions *i)* and *ii)* contain leading terms (quadratic in the large logarithms L_0, L_Q), whereas region *iii)* contains formally nonleading terms of order $L_0 \ln(1/\theta_0^2)$, which, however, give a contribution numerically larger than the leading ones since $\varepsilon\theta_0/m \ll 1/\theta_0$.

The calculation beyond the leading logarithmic approximation may be performed using the results of a paper of one of us [48]. The contribution from the kinematical region *i)* (with both hard photons being tagged), has the form (see Eq. (Π 6) from [48]):

$$
\frac{z}{y}\frac{\mathrm{d}^3\sigma_i^{\gamma\gamma}}{\mathrm{d}x\,\mathrm{d}y\,\mathrm{d}z} = \frac{\alpha^2}{8\pi^2}L_0\left[L_0\left(P_\Theta^{(2)}(z) + 2\frac{1+z^2}{1-z}\left(\ln z - \frac{3}{2} - 2\ln\Delta\right)\right) + \right.
$$
$$
\left. + 6(1-z) + \left(\frac{4}{1-z} - 1 - z\right)\ln^2 z - 4\frac{(1+z)^2}{1-z}\ln\frac{1-z}{\Delta}\right]\tilde{\Sigma} + O(1). \quad (1.2.17)
$$

Here we use the notation $P_\Theta^{(2)}(z)$ for the Θ part of the second order term of the expansion of the electron nonsinglet structure function,

$$
\begin{aligned}
D(z, L) &= \delta(1-z) + \frac{\alpha}{2\pi}P^{(1)}(z)L + \frac{1}{2}\left(\frac{\alpha}{2\pi}\right)^2 P^{(2)}(z)L^2 + \dots \quad (1.2.18)\\
P^{(i)}(z) &= P_\Theta^{(i)}(z)\Theta(1-z-\Delta) + P_\delta^{(i)}\delta(1-z), \quad \Delta \to 0,\\
P_\Theta^{(1)}(z) &= \frac{1+z^2}{1-z}, \quad P_\delta^{(1)} = \frac{3}{2} + 2\ln\Delta,\\
P_\Theta^{(2)}(z) &= 2\left[\frac{1+z^2}{1-z}\left(2\ln(1-z) - \ln z + \frac{3}{2}\right) + \frac{1}{2}(1+z)\ln z - 1 + z\right].
\end{aligned}
$$

The parameter Δ serves as the infrared regularization parameter.

The contribution of the kinematical region *ii)* to the observed cross section depends on the event selection; in other words, on the method of measurement of the scattered particles.

In the case of exclusive event selection, when only the scattered electron is detected, while the photon that is emitted almost collinearly (i.e., within a small cone with opening angle $2\theta'_0$ around the momentum of the outgoing electron) goes unnoticed or is not taken into account in the determination of the kinematical variables, we have (see Π8 from [48])

$$
\frac{z}{y}\frac{\mathrm{d}^3\sigma_{ii}^{\gamma\gamma}}{\mathrm{d}x\,\mathrm{d}y\,\mathrm{d}z} = \frac{\alpha^2}{4\pi^2}P(z,L_0)\int\limits_{\Delta/Y}^{y_2^{\mathrm{max}}}\frac{\mathrm{d}y_2}{1+y_2}\left[\frac{1+(1+y_2)^2}{y_2}(\widetilde{L}-1)+y_2\right]\Sigma_s,
$$

$$
\Sigma_s = \Sigma(x_b, y_b, Q_b^2), \tag{1.2.19}
$$

where

$$
\widetilde{L} = \ln\left(\frac{\varepsilon\theta'_0}{m}\right)^2 + 2\ln Y, \quad y_2 = \frac{x_2}{Y}, \quad Y = \frac{\varepsilon_2}{\varepsilon}, \quad y_2^{\mathrm{max}} = \frac{2z - Y(1+c)}{Y(1+c)},
$$

$$
x_b = \frac{xyz(1+y_2)}{z-(1-y)(1+y_2)}, \quad y_b = \frac{z-(1-y)(1+y_2)}{z}, \quad Q_b^2 = Q^2 z(1+y_2). \tag{1.2.20}
$$

More realistic (from the experimental point of view) is the calorimetric event selection, when only the sum of the energies of the outgoing electron and photon can be measured if the photon momentum lies inside the small cone with opening angle $2\theta'_0$ along the direction of the final electron. In this case we find

$$
\frac{z}{y}\frac{\mathrm{d}^3\sigma_{ii,\mathrm{cal}}^{\gamma\gamma}}{\mathrm{d}x\,\mathrm{d}y\,\mathrm{d}z} = \frac{\alpha^2}{4\pi^2}P(z,L_0)\int\limits_{\Delta/Y}^{\infty}\frac{\mathrm{d}y_2}{(1+y_2)^3}\left[\frac{1+(1+y_2)^2}{y_2}(\widetilde{L}-1)+y_2\right]\widetilde{\Sigma} =
$$

$$
= \frac{\alpha^2}{4\pi^2}P(z,L_0)\left[(\widetilde{L}-1)\left(2\ln\frac{Y}{\Delta}-\frac{3}{2}\right)+\frac{1}{2}\right]\widetilde{\Sigma}. \tag{1.2.21}
$$

In the last equation we used the relation

$$
\Sigma_s = \frac{1}{(1+y_2)^2}\widetilde{\Sigma}, \tag{1.2.22}
$$

which is valid for the calorimetric set-up.

Consider at last the semicollinear region *iii)*. The relevant contribution may be calculated using the quasireal electron method [49]:

$$
\frac{z}{y}\frac{\mathrm{d}^3\sigma_{iii}^{\gamma\gamma}}{\mathrm{d}x\,\mathrm{d}y\,\mathrm{d}z} = \frac{\alpha}{2\pi}P(z,L_0)\frac{2\alpha}{\pi}\int\frac{\mathrm{d}^3k_2}{\omega_2}\frac{\alpha^2(Q_{sc}^2)}{Q_{sc}^4}I^\gamma, \quad I^\gamma = B_{\rho\sigma}(zp_1,p_2,k_1)\frac{H^{\rho\sigma}}{8\pi}. \tag{1.2.23}
$$

The quantity $B_{\rho\sigma}(zp_1, p_2, k_1)$ is obtained from equation (1.2.11), where it is necessary to set $m = 0$. After some algebraic transformations we obtain

$$I^\gamma = \frac{1}{st}\left[F_2(x_{sc}, Q_{sc}^2)\left(\frac{M^2}{Q_{sc}^2}x_{sc}G - V\Big[x_{sc}(z^2 + (1-y)^2)V + (1-y)(zQ^2-s) - \right.\right.$$

$$\left.\left. - z(zQ^2 - t)\Big]\right) - GF_1(x_{sc}, Q_{sc}^2)\right], \qquad G = z^2Q^4 - 2st + Q_{sc}^4, \qquad (1.2.24)$$

$$x_{sc} = \frac{Q_{sc}^2}{V(z + y - 1) - 2P \cdot k_2}, \quad s = 2p_2 \cdot k_2, \quad t = -2zp_1 \cdot k_2,$$

$$Q_{sc}^2 = zQ^2 - s - t.$$

The angular integration in Eq. (1.2.23) is to be performed over the whole phase space, excepting the small cones along directions of motion of the initial and scattered electrons that correspond to the kinematic regions *i)* or *ii)*. The result (for details see Appendix G) has the form:

$$\frac{z}{y}\frac{\mathrm{d}^3\sigma_{iii}^{\gamma\gamma}}{\mathrm{d}x\,\mathrm{d}y\,\mathrm{d}z} = \left(\frac{\alpha}{2\pi}\right)^2 P(z, L_0)\left[\int_\Delta^{x_2^t}\frac{\mathrm{d}x_2}{x_2}\frac{z^2 + (z-x_2)^2}{z(z-x_2)}\ln\frac{2(1-c)}{\theta_0^2}\Sigma_t + \right.$$

$$\left. + \int_\Delta^{x_2^s}\frac{\mathrm{d}x_2}{x_2}\frac{1 + (1+y_2)^2}{1+y_2}\ln\frac{2(1-c)}{\theta_0'^2}\Sigma_s + Z\right], \qquad (1.2.25)$$

$$\Sigma_t = \Sigma(x_t, y_t, Q_t^2),$$

The logarithmic dependences on the infrared regulator Δ and on the angles θ_0, θ_0' are fully contained in the first two terms on the r.h.s., whereas the quantity Z represents an integral over the whole photon phase space of a well-behaved function, and it is free from collinear and infrared singularities. Its explicit expression is given in Appendix G.

The upper limits of the x_2 integration in (1.2.25) read

$$x_2^t = z - \frac{Y(1+c)}{2}, \qquad x_2^s = \frac{2z - Y(1+c)}{1+c}, \qquad (1.2.26)$$

and the arguments of Σ_t are

$$x_t = \frac{xy(z - x_2)}{z - x_2 + y - 1}, \quad y_t = \frac{z - x_2 + y - 1}{z - x_2}, \quad Q_t = Q^2(z - x_2). \quad (1.2.27)$$

An explicit expression for x_m, which is relevant for the calculation of Z, is given in Appendix G.

The formulae given above (see Eqs. (1.2.7), (1.2.16), (1.2.17), (1.2.19) or (1.2.21), and (1.2.25)) provide the complete answer for the leading and subleading contributions up to the second order of perturbation theory. The total sum of virtual, soft, and hard additional photons emission corrections to the radiative DIS cross section does not depend on the auxiliary parameter $\Delta = \delta\varepsilon/\varepsilon$, as it should be.

1.2.3. Results for Different Experimental Set-Ups. The sum of the contributions of the leading and next-to-leading corrections at order α^2, which are given explicitly in the expressions (1.2.16), (1.2.17), (1.2.19) or (1.2.21), and (1.2.25), may be written in the form

$$\frac{z}{y}\frac{\mathrm{d}^3\sigma}{\mathrm{d}x\,\mathrm{d}y\,\mathrm{d}z} = \left(\frac{\alpha}{2\pi}\right)^2 (\Sigma_i + \Sigma_f)\,. \tag{1.2.28}$$

The first term Σ_i is independent of the experimental selection of the scattered electron and has the form:

$$
\begin{aligned}
\Sigma_i &= \left\{\frac{1}{2}L_0^2 P_\Theta^{(2)}(z) + P(z, L_0)\left[\frac{1 - 16z - z^2}{2(1 + z^2)} + \left(3 - 2\ln Y + \frac{4z}{1 + z^2}\right)\ln z + \right.\right. \\
&\quad + \ln^2 Y - 2\mathrm{Li}_2(z) + 2\mathrm{Li}_2\left(\frac{1 + c}{2}\right) - \frac{2(1 + z)^2}{1 + z^2}\ln(1 - z) + \\
&\quad + \left.\left.\frac{1 - z^2}{2(1 + z^2)}\ln^2 z\right]\right\}\tilde{\Sigma} + P(z, L_0)\,\tilde{\Sigma}\,\ln\frac{2(1 - c)}{\theta_0^2}\left[\int_0^{u_0}\frac{\mathrm{d}u}{u}(1 + (1 - u)^2)\times\right. \\
&\quad \times \left.\left(\frac{\Sigma_t}{(1 - u)\tilde{\Sigma}} - 1\right) - \int_{u_0}^1\frac{\mathrm{d}u}{u}(1 + (1 - u)^2)\right] + P(z, L_0)\,Z, \tag{1.2.29}
\end{aligned}
$$

$$u = \frac{x_2}{z}, \qquad u_0 = \frac{x_2^t}{z},$$

where Z is given in Appendix G and the remaining notations are as above (see (1.2.17), (1.2.24), and (1.2.26)).

The second term in (1.2.28), denoted Σ_f, however, does explicitly depend on the event selection. It corresponds to the emission of a hard photon by the scattered electron. In the exclusive set-up, when only the scattered bare electron is measured, while the photon that is emitted close to the final electron's direction

is ignored, this contribution reads

$$\Sigma_f = \Sigma_f^{\text{excl}} = P(z, L_0) \int\limits_0^{x_2^s/Y} \mathrm{d}y_2 \left[\left(\frac{1 + (1 + y_2)^2}{y_2} (L_Q + \ln Y - 1) + y_2 \right) \frac{1}{1 + y_2} \times \right.$$

$$\left. \times \Theta \left(y_2 - \frac{\Delta}{Y} \right) + (L_Q + \ln Y - 1)\delta(y_2) \left(2 \ln \frac{\Delta}{Y} + \frac{3}{2} \right) \right] \Sigma_s. \qquad (1.2.30)$$

In this case the parameter θ_0', that separated the kinematic regions *ii)* and *iii)*, only plays the role of an auxiliary one; it has already cancelled in the above expression for the cross section.

As we will see below, this situation is quite different for the experimentally more realistic, calorimetric set-up, when the detector cannot distinguish between events with a bare electron and events when the electron is accompanied by a hard photon emitted within a small cone with opening angle $2\theta_0'$ around the direction of the scattered electron. For this case we obtain

$$\Sigma_f = \Sigma_f^{\text{cal}} = P(z, L_0) \left[\frac{1}{2} \tilde{\Sigma} + \ln \frac{2(1 - c)}{\theta_0'^2} \int\limits_0^\infty \frac{\mathrm{d}y_2}{y_2} \frac{1 + (1 + y_2)^2}{1 + y_2} \times \right.$$

$$\left. \times \left(\Sigma_s \Theta(y_2^{\max} - y_2) - \frac{\tilde{\Sigma}}{(1 + y_2)^2} \right) \right]. \qquad (1.2.31)$$

For the calorimetric event selection the parameter θ_0' is a physical one and the final result therefore does depend on it. However, the mass singularity that is connected with the emission of the photon off the scattered electron is cancelled in accordance with the Kinoshita–Lee–Nauenberg theorem [50].

Note that the case of a coarse detector for the scattered electron, i.e., $\theta_0' \sim$ $\sim O(1)$, agrees at the level of leading logarithms with the result of paper [51], that was obtained in the approximation of absence of emission along the scattered electron. Our result disagrees with the result of Bardin et al. [42] on the radiative corrections, as they neglected the interference of the emission of two photons; see [51] for a detailed discussion.

We note in conclusion that the set of Feynman diagrams considered here is gauge invariant and model independent but not complete. We have neglected the contributions with two virtual photons exchanged between electron and the target that appear at the same order of perturbation theory, as well as the interference with the contributions when the second photon is emitted by the hadronic side. However, the description of this part is definitely model dependent. The details and the numerical estimates may be found in [52].

1.3. Compton Tensor with Heavy Photon in the Case of Longitudinally Polarized Fermion. Here we shall restrict our consideration to the part of the Compton tensor, which contains the degree of polarization of the initial electron [53]. Our aim is to calculate soft and virtual QED radiative corrections to the tensor. The corrections are important for modern precise experiments in DIS. Possible applications of our results will be considered in Conclusions.
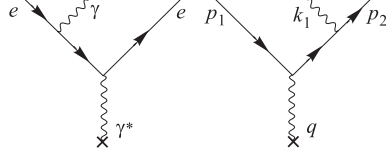
Fig. 1. The Born-level Feynman diagrams

Let us consider the process (see Fig. 1)

$$\gamma^*(q) \ + \ e(p_1) \ \longrightarrow \ \gamma(k_1) \ + \ e(p_2), \tag{1.3.1}$$

$$q^2 < 0, \qquad k_1^2 = 0, \qquad p_1^2 = p_2^2 = m^2, \qquad p_1 + q = p_2 + k_1,$$

where m is the electron mass.

The Compton tensor is defined as

$$K_{\rho\sigma} = (8\pi\alpha)^{-2}\Sigma M_\rho^{e\gamma^*\to e\gamma}(M_\sigma^{e\gamma^*\to e\gamma})^*. \tag{1.3.2}$$

Here the matrix element M describes the Compton scattering process (1.3.1),

$$M_\rho = M_{0\rho} + M_{1\rho} = \bar{u}(p_2)O_{\rho\mu}u(p_1)e^\mu(k_1),$$

$$O_{\rho\mu} = O_{\rho\mu}^{(0)} + \frac{\alpha}{4\pi}O_{\rho\mu}^{(1)}, \quad O_{\rho\mu}^{(0)} = \gamma_\rho\frac{\hat{p}_2 - \hat{q} + m}{t}\gamma_\mu + \gamma_\mu\frac{\hat{p}_1 + \hat{q} + m}{s}\gamma_\rho,$$

$$s = 2p_2k_1, \qquad t = -2p_1k_1. \tag{1.3.3}$$

Quantities $O_{\rho\mu}^{(0)}$ and $O_{\rho\mu}^{(1)}$ take into account the lowest and the first orders of perturbation theory, respectively. Here and in what follows, we use the following notation for scalar products of 4-vectors:

$$\hat{a} = \gamma_\mu a^\mu, \qquad ab = a_\mu b^\mu = a^0 b^0 - \mathbf{ab},$$

and the polarization vector of the real photon is $e^\mu(k_1)$.

1.3.1. Radiative Corrections. Calculating the first order correction, we assume that all kinematical invariants of the process are large in comparison with the electron mass square:

$$s \sim -t \sim -u \sim -q^2 \gg m^2, \qquad u = -2p_1p_2, \qquad q^2 = s + t + u. \tag{1.3.4}$$

So, we will neglect the electron mass in all places, where it is possible. Note that for the unpolarized case in [33] the mass was taken into account.

The Compton tensor, defined in (1.3.2), is hermitian:

$$K_{\rho\sigma} = K_{\sigma\rho}^*. \tag{1.3.5}$$

We shall separate the contributions, associated with the electron polarization:

$$K_{\rho\sigma} = K_{\rho\sigma}^0 + \frac{\alpha}{4\pi}\left(K_{\rho\sigma}^1 + K_{\sigma\rho}^{1*}\right), \tag{1.3.6}$$

$$K_{\rho\sigma}^0 = B_{\rho\sigma} + \xi P_{\rho\sigma}^0, \qquad K_{\rho\sigma}^1 = T_{\rho\sigma} + \xi P_{\rho\sigma}^1,$$

where ξ is the degree of the initial electron polarization. Quantities $B_{\rho\sigma}$ and $T_{\rho\sigma}$ correspond to the case of unpolarized electron,

$$B_{\rho\sigma} = B_g \tilde{g}_{\rho\sigma} + B_{11}\tilde{p}_{1\rho}\tilde{p}_{1\sigma} + B_{22}\tilde{p}_{2\rho}\tilde{p}_{2\sigma}, \tag{1.3.7}$$

$$B_g = \frac{1}{st}[(s+u)^2 + (t+u)^2] - 2m^2q^2\left(\frac{1}{s^2} + \frac{1}{t^2}\right),$$

$$B_{11} = \frac{4q^2}{st} - \frac{8m^2}{s^2}, \qquad B_{22} = \frac{4q^2}{st} - \frac{8m^2}{t^2}.$$

The new variables

$$\tilde{g}_{\rho\sigma} = g_{\rho\sigma} - \frac{q_\rho q_\sigma}{q^2}, \qquad \tilde{p}_{1\rho} = p_{1,2}^\rho - \frac{p_{1,2}q}{q^2}q^\rho \tag{1.3.8}$$

provide the explicit fulfillment of gauge conditions: $q_\rho K^{\rho\sigma} = 0$, $q_\sigma K^{\rho\sigma} = 0$. Quantity $T_{\rho\sigma}$ has a rather cumbersome form, it is given in [33].

For the case of the most general form of the electron polarization vector

$$u(p)\bar{u}(p) = (\hat{p}_1 + m)(1 - \xi\gamma_5\hat{a}) \tag{1.3.9}$$

one obtains (see also [11, 12])

$$P_{\rho\sigma}^0 = 4m\left\{(p_1 q\rho\sigma)\frac{qa - 2p_2 a}{st} + (p_2 q\rho\sigma)\left[\frac{qa}{t^2} + \frac{p_2 a}{t}\left(\frac{1}{s} - \frac{1}{t}\right)\right] + \right.$$

$$\left. + \ (qa\rho\sigma)\left[\frac{q^2}{st} - \frac{1}{s} - \frac{1}{t} - m^2\left(\frac{1}{s^2} + \frac{1}{t^2}\right)\right]\right\}, \tag{1.3.10}$$

where we used the notation

$$(abcd) \equiv i\varepsilon_{\alpha\beta\gamma\delta}a^\alpha b^\beta c^\gamma d^\delta. \tag{1.3.11}$$

The above object obeys the Shouten identity:

$$(abcd)ef = (fbcd)ae + (afcd)be + (abfd)ce + (abcf)de. \tag{1.3.12}$$

In this part we shall consider only the case of longitudinally polarized fermion:

$$u(p_1)\bar{u}(p_1) = \hat{p}_1(1 - \xi\gamma_5). \tag{1.3.13}$$

This is the most interesting case for physical applications. In the Born approximation we obtain

$$
\begin{aligned}
P_{\rho\sigma} &= \xi\left[P^0_{\rho\sigma} + \frac{\alpha}{4\pi}P^1_{\rho\sigma}\right], \tag{1.3.14}\\
P^0_{\rho\sigma} &= P^{0t}_{\rho\sigma} + P^{0s}_{\rho\sigma} = \frac{2}{st}\left[(u+t)(p_1q\rho\sigma) + (u+s)(p_2q\rho\sigma)\right].
\end{aligned}
$$

Here and below the upper indices t and s denote the contributions of Feynman diagrams with real photon emission from the initial and final electron lines, respectively. Using the explicit expressions for $P^{0t,s}_{\rho\sigma}$, it is easy to check the following relations:

$$q_\rho P^0_{\rho\sigma} = q_\sigma P^0_{\rho\sigma} = 0, \ (P^{0s,t}_{\sigma\rho})^* = P^{0s,t}_{\rho\sigma}, \ P^{0s,t}_{\rho\sigma}q_\rho = 0, \ P^{0s,t}_{\rho\sigma}q_\sigma \neq 0, \tag{1.3.15}$$

$$
\begin{aligned}
P^{0t}_{\rho\sigma} &= \frac{1}{st}\Bigg[4(p_1p_2q\sigma)(p_{1\rho} + p_{2\rho}) + \\
&\qquad + 2(t-s)(p_1p_2\rho\sigma) + 2(s+u)(p_2q\rho\sigma)\Bigg], \\
P^{0s}_{\rho\sigma} &= \frac{1}{st}\Bigg[-4(p_1p_2q\sigma)(p_{1\rho} + p_{2\rho}) + \\
&\qquad + 2(s-t)(p_1p_2\rho\sigma) + 2(s+t)(p_1q\rho\sigma)\Bigg].
\end{aligned}
\tag{1.3.16}
$$

Note now, that we may consider only a half of the full set of eight one-loop Feynman diagrams. Namely, we take the t-type diagrams with real photon emission from the *initial* electron line (Fig. 2). To get the first order correction, we multiply the amplitudes of the one-loop graphs by the Born ones. The whole contribution (including the impact of the rest four one-loop diagrams) can be obtained, using the rearrangement ($\hat{H}$) and hermitization ($\hat{H}$) operators:

$$P^1_{\rho\sigma} = (1 + \hat{H})(1 - \hat{P})(P^{a,b} + P^{1c} + P^{1d})_{\rho\sigma} + P^{\text{soft}}_{\rho\sigma}, \tag{1.3.17}$$

where the operators are defined as follows:

$$\hat{P}F(\rho, \sigma, p_1, p_2, q, s, t) = F(\rho, \sigma, p_2, p_1, -q, t, s), \qquad \hat{H}a_{\rho\sigma} = a^*_{\sigma\rho}. \tag{1.3.18}$$
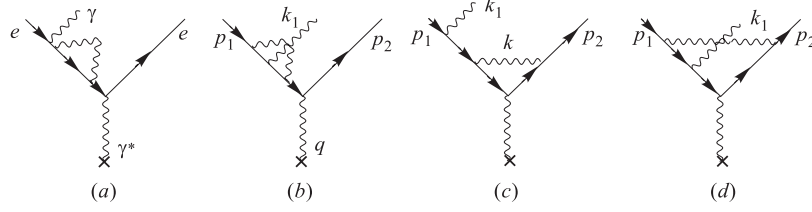
Fig. 2. One-loop virtual Feynman diagrams with photon emission by the *initial* electron

Note, that $\hat{P}P_{\rho\sigma}^{0s,t} = -P_{\rho\sigma}^{0t,s}$. The last term in Eq.(1.3.17) describes the contribution, coming from emission of an additional soft photon [33]:

$$P_{\rho\sigma}^{\text{soft}} = P_{\rho\sigma}^0 \delta^{\text{soft}}, \tag{1.3.19}$$

$$\delta^{\text{soft}} = -\frac{4\pi\alpha}{16\pi^3} \int \frac{d^3k}{\omega} \left(\frac{p_1}{p_1 k} - \frac{p_2}{p_2 k} \right)^2 =$$

$$= \frac{\alpha}{\pi} \left[(L_u - 1) \ln \frac{m^2 (\Delta\varepsilon)^2}{\lambda^2 \varepsilon_1 \varepsilon_2} + \frac{1}{2} L_u^2 - \frac{1}{2} \ln^2 \frac{\varepsilon_1}{\varepsilon_2} - \frac{\pi^2}{3} + \text{Li}_2 \left(1 + \frac{u}{4\varepsilon_1 \varepsilon_2} \right) \right],$$

$$L_u = \ln \frac{-u}{m^2}, \qquad \text{Li}_2(z) = -\int\limits_0^1 \frac{dx}{x} \ln(1 - zx).$$

Here $\Delta\varepsilon$ is the maximal energy of soft photon; quantities $\varepsilon_{1,2} = p_{1,2}^0$ are the energies of the initial and the final electrons in the laboratory reference frame (in the rest reference frame of the target).

Considering the matrix elements of the Feynman graphs Fig. 2,a,b, we get

$$(M_\sigma^a + M_\sigma^b)(-i(4\alpha\pi)^2)^{-1} = \frac{\alpha}{2\pi} \bar{u}(p_2)\gamma_\sigma \left[mN_1 \left(\hat{e} - \hat{k}_1 \frac{p_1 e}{p_1 k_1} \right) + N_2 \hat{k}_1 \hat{e} \right] u(p_1),$$

$$N_1 = \frac{1}{2(t + m^2)} \left[1 - \frac{t}{t + m^2} L_t \right], \tag{1.3.20}$$

$$N_2 = \frac{1}{2(t + m^2)} - \frac{2t^2 + 3m^2 t + 2m^4}{2t(t + m^2)^2} L_t + \frac{m^2}{t^2} \left[-\text{Li}_2 \left(1 + \frac{t}{m^2} \right) + \frac{\pi^2}{6} \right].$$

One can see that only the structure in front of coefficient N_2 survives in the limit $m \to 0$. Really, the trace of the product of Dirac matrices, associated with N_1, has an odd number of matrices and gives an extra power of the mass. We would like to note that in the case of photon emission at small angles (which is not

under consideration now) the situation with the limit $m \to 0$ is more subtle and requires a special investigation (see [54], for instance).

After a simple algebraic transformation we get

$$P^{a,b}_{\rho\sigma} = 2 \frac{2L_t - 1}{st} [2(p_1 p_2 q \sigma) p_{2\rho} + (u + s)((p_2 q \rho \sigma) - (p_1 p_2 \rho \sigma))]. \quad (1.3.21)$$

The remaining contributions (see Fig. 2,c,d) are

$$P^{1c}_{\rho\sigma} = \frac{1}{t} \int \frac{\mathrm{d}^4 k}{\mathrm{i}\pi^2} \frac{1}{a_0 a_2 a_q} \frac{1}{4} \mathrm{Tr} \{\hat{p}_2 \gamma_\lambda (\hat{p}_2 - \hat{k}) \gamma_\sigma (\hat{p}_2 - \hat{q} - \hat{k}) \gamma_\lambda (\hat{p}_2 - \hat{q}) \gamma_\mu \hat{p}_1 \gamma_5 \tilde{O}^0_{\rho\mu}\} \quad (1.3.22)$$

and

$$P^{1d}_{\rho\sigma} = \int \frac{\mathrm{d}^4 k}{\mathrm{i}\pi^2} \frac{1}{a_0 a_1 a_2 a_q} \frac{1}{4} \mathrm{Tr} \{\hat{p}_2 \gamma_\lambda (\hat{p}_2 - \hat{k}) \gamma_\sigma (\hat{p}_2 - \hat{q} - \hat{k}) \gamma_\mu (\hat{p}_1 - \hat{k}) \gamma_\lambda \hat{p}_1 \gamma_5 \tilde{O}^0_{\rho\mu}\}, \quad (1.3.23)$$

where

$$\begin{aligned} a_0 &= k^2 - \lambda^2, & a_1 &= k^2 - 2p_1 k, \\ a_2 &= k^2 - 2p_2 k, & a_q &= (p_2 - q - k)^2 - m^2. \end{aligned} \quad (1.3.24)$$

The matrix $\tilde{O}^0_{\rho\mu}$ differs from $O^0_{\rho\mu}$ (see Eq. (1.3.3)) by the reversal order of gamma matrices. Using the Table of integrals given in [53], one can perform the integration over the loop momentum in the right-hand sides of the expressions for P^{1c}, P^{1d}, and obtain the total expression for the Compton tensor. Its explicit form is given below.

Now we concentrate on the terms, which contain infrared singularities. There are three sources of them. The first one is the renormalization constant

$$Z_1 = 1 - \frac{\alpha}{2\pi}\left(\frac{1}{2}L_\Lambda + 2\ln\frac{\lambda}{m} + \frac{9}{4}\right), \quad L_\Lambda = \ln\frac{\Lambda^2}{m^2}, \quad (1.3.25)$$

which is required to remove the ultraviolet divergence of the vertex function, appearing in P^{1c}. The next source is a part of the box contribution P^{1d}, which comes from scalar loop integrals. Really, for the Feynman diagram Fig. 2,d the infrared terms are associated with the integral

$$I = \int \frac{\mathrm{d}^4 k}{\mathrm{i}\pi^2} \frac{1}{a_0 a_1 a_2 a_q} =$$
$$= \frac{1}{tu}\left[2L_u \ln\frac{m}{\lambda} - L_q^2 + 2L_t L_u - \frac{\pi^2}{6} - 2\mathrm{Li}_2(1 - \frac{q^2}{u})\right], \quad (1.3.26)$$
$$L_q = \ln\frac{-q^2}{m^2}, \qquad L_t = \ln\frac{-t}{m^2}.$$

The third source is the emission of additional soft photons, which was considered above. The infrared singularities are cancelled out in the total sum.

Let us consider the contribution from one-loop corrections

$$P^t_{\rho\sigma} = (P^{a,b} + P^{1c} + P^{1d})_{\rho\sigma}. \tag{1.3.27}$$

Extracting the leading logarithmic terms and infrared singularities, we can present it as follows:

$$P^t_{\rho\sigma} = P^{0t}_{\rho\sigma}\left[-L^2_u - 4(L_u - 1)\ln\frac{m}{\lambda} + 3L_u\right] + R^t_{\rho\sigma}. \tag{1.3.28}$$

After the hermitization and rearrangement operations, and adding the soft photon contribution, we come to the result

$$P_{\rho\sigma} = P^0_{\rho\sigma}\left\{1 + \frac{\alpha}{\pi}\left[(L_u - 1)\ln\frac{(\Delta\varepsilon)^2}{\varepsilon_1\varepsilon_2} + \frac{3}{2}L_u - \frac{1}{2}\ln^2\frac{\varepsilon_2}{\varepsilon_1} - \right.\right.$$
$$\left.\left. - \frac{\pi^2}{3} + \mathrm{Li}_2(\cos^2\frac{\theta}{2})\right]\right\} + \frac{\alpha}{4\pi}R_{\rho\sigma}. \tag{1.3.29}$$

Quantities $R^t_{\rho\sigma}$ and $R_{\rho\sigma}$ collect nonleading terms. They are free from infrared singularities.

Tensor $R^t_{\rho\sigma}$ can be presented in the form

$$R^t_{\rho\sigma} = A(2q\sigma\rho) + B(1q\sigma\rho) + C(12q\sigma)p_{1\rho} + D(12q\sigma)p_{2\rho} +$$
$$+ E(12q\sigma)q_\rho + F(12\sigma\rho). \tag{1.3.30}$$

The coefficients $A - F$ have a rather cumbersome form, we do not present them here. Note only that they obey the condition

$$Cp_1q + Dp_2q + Eq^2 - F = 0, \tag{1.3.31}$$

because of gauge invariance in respect to index ρ.

The rearrangement operation gives

$$\begin{aligned}(1 - \hat{P})R^t_{\rho\sigma} &= (A + \tilde{B})(2q\sigma\rho) + (B + \tilde{A})(1q\sigma\rho) + (C - \tilde{D})(12q\sigma)p_{1\rho} + \\ &+ (D - \tilde{C})(12q\sigma)p_{2\rho} + (E + \tilde{E})(12q\sigma)q_\rho + (F + \tilde{F})(12\sigma\rho) \equiv \\ &\equiv A_1(1q\sigma\rho) + A_2(2q\sigma\rho) + B_1(12q\sigma)p_{1\rho} + B_2(12q\sigma)p_{2\rho} + \\ &+ C_1(12q\sigma)q_\rho + F_1(12\sigma\rho). \end{aligned} \tag{1.3.32}$$

Tests of the gauge invariance is an important check of our calculations:

$$q^\rho(1 - \hat{P})R_{\rho\sigma} = B_1(12q\sigma)p_1q + B_2(12q\sigma)p_2q + C_1(12q\sigma)q^2 + F_1(12\sigma q) = 0,$$
$$q^\sigma(1 - \hat{P})R_{\rho\sigma} = F_1(12q\rho) = 0. \tag{1.3.33}$$

These conditions yield

$$F_1 = 0, \qquad C_1 = -B_1 \frac{p_1 q}{q^2} - B_2 \frac{p_2 q}{q^2},$$

$$B_1 p_{1\rho} + B_2 p_{2\rho} + C_1 q_\rho = B_1 \tilde{p}_{1\rho} + B_2 \tilde{p}_{2\rho}, \qquad (1.3.34)$$

$$\tilde{p}_{1\rho} = p_{1\rho} - \frac{p_1 q}{q^2} q_\rho, \quad \tilde{p}_{2\rho} = p_{2\rho} - \frac{p_2 q}{q^2} q_\rho.$$

We checked these relations by straightforward calculations.

The last step is the hermitization, which gives

$$
\begin{aligned}
R_{\rho\sigma} &= (1 + \hat{H})(1 - \hat{P}) R^t_{\rho\sigma} = \\
&= (A_1 + A_1^*)(1 q \sigma \rho) + (A_2 + A_2^*)(2 q \sigma \rho) + \\
&+ (12 q \sigma)[B_1 \tilde{p}_{1\rho} + B_2 \tilde{p}_{2\rho}] - (12 q \rho)[B_1^* \tilde{p}_{1\sigma} + B_2^* \tilde{p}_{2\sigma}], \quad (1.3.35)
\end{aligned}
$$

where

$$
\begin{aligned}
A_1 &= \frac{2}{st}\left[\frac{2u(2s-u)}{a} L_{qu} + \frac{4us}{a}\left(\frac{u}{a} L_{qu} - 1\right) + \frac{ub}{c} + \frac{2u^2 + us - s^2}{c} L_{sq} + \right. \\
&+ \left. \frac{usb}{c^2} L_{sq} - 2c\zeta(2) - 2c L_{tu} + (2s - c) L_{qu} - \frac{uc}{s} G + \left(\frac{ub}{t} + c\right)\tilde{G} + 5c - 2s \right],
\end{aligned}
$$

$$
\begin{aligned}
B_1 &= \frac{2}{st}\left[\frac{8u}{a}\left(1 - \left(\frac{u}{a} + 1\right) L_{qu}\right) + \frac{6t}{b} L_{qt} + \frac{2(u^2 - 2s^2 - su)}{cu} L_{sq} + \right. \\
&+ \frac{2b}{c}\left(1 + \frac{s}{c} L_{sq}\right) + \frac{2}{s}(2c - s) L_{tu} + \left(-2 - \frac{4c^2}{st} - \frac{12b}{t} - \frac{4s^2}{ut}\right) L_{qu} + \\
&+ \left. \frac{4b^2}{tu} L_{su} + \left(-2 + \frac{2uc}{s^2} - \frac{2t}{s}\right) G + \left(\frac{2b}{t} + \frac{2b^2}{t^2}\right)\tilde{G} + 6 \right],
\end{aligned}
$$

$$
G = (L_q - L_u)(L_q + L_u - 2L_t) - \frac{\pi^2}{3} - 2\mathrm{Li}_2\left(1 - \frac{q^2}{u}\right) + 2\mathrm{Li}_2\left(1 - \frac{t}{q^2}\right),
$$

$$
A_2 = (s \leftrightarrow t) A_1, \qquad B_2 = -(s \leftrightarrow t) B_1, \qquad \tilde{G} = (s \leftrightarrow t) G. \qquad (1.3.36)
$$

Note, that the above expressions are free from kinematical singularities. Really, in the limits $a \to 0$, $b \to 0$, and $c \to 0$ the quantities are finite. The symmetry between A_1, B_1 and A_2, B_2 takes place due to the initial symmetry between p_1 and p_2 in the traces.

1.3.2. Conclusions. Thus we calculated the part of the leptonic tensor, proportional to the degree of the initial longitudinal polarization. This tensor describes Compton scattering with one off-shell photon, which is related to a certain target. The main results of the paper are presented by Eqs.(1.3.29),(1.3.35).

The calculation allows one to obtain corrections, coming from one-loop effects, to quantities observable in different polarization experiments. Let us consider for definiteness the task of calculation of α^2 order radiative correction in polarized deep inelastic scattering. The results for the lowest order QED correction for nucleon and nuclear targets can be found in Refs. 11, 12. Both the Born cross section (σ_{Born}) and the cross section at the level of radiative corrections (σ_{RC}) can be split into unpolarized and polarized parts:

$$\sigma_{\text{Born,RC}} = \sigma^{\text{unp}}_{\text{Born,RC}} + \xi_b \xi_t \sigma^{\text{pol}}_{\text{Born,RC}}, \tag{1.3.37}$$

where ξ_b and ξ_t are polarization degrees of the beam and target. The correction to asymmetry ($A = \sigma^{\text{pol}}/\sigma^{\text{unp}}$)

$$\Delta A = \frac{\sigma^{\text{pol}}_{\text{RC}} \sigma^{\text{unp}}_{\text{Born}} - \sigma^{\text{unp}}_{\text{RC}} \sigma^{\text{pol}}_{\text{Born}}}{\sigma^{\text{unp}}_{\text{Born}} (\sigma^{\text{unp}}_{\text{Born}} + \sigma^{\text{unp}}_{\text{RC}})} \tag{1.3.38}$$

is usually not large because of mutual cancellation of large factorizing terms. It is clear, that when a relatively small correction is obtained as a difference of two large terms, the radiatively corrected cross section has to be calculated with the most possible accuracy, and a special attention has to be paid to nonfactorizing terms like (1.3.36). The kinematical regions with very high y ($y \sim 0.9$) can be reachable in the current polarization experiments in DIS [55, 56]. In this region radiative corrections to the cross section are comparable with the Born cross section. Basically, it comes from the contributions of radiative tails from elastic and quasielastic peaks. This calculation firstly allows one to obtain the contribution of these tails with taking into account loop effects in the next-to-leading approximation.

Strictly speaking, the total QED correction $\sim \alpha^2$ to spin asymmetry Eq.(1.3.38) includes also contributions of double bremsstrahlung, lepton pair production and two-loop virtual corrections. The latter does not change kinematics of the general process, it can be easily derived using the results of Ref. 57. The leading contribution of two-loop corrections is factorized in front of the Born cross section, and it is exactly cancelled in the numerator of (1.3.38). Contrary, the radiative process has a different kinematics; and it is of particular interest in experiments. So, the elastic and quasielastic radiative tails, which have relatively large cross section, provide an important correction to polarized and unpolarized DIS. The contributions of double bremsstrahlung and lepton pair production can be calculated using analytical or Monte Carlo approach. We note that there are no infrared divergences in the case of correction to elastic and quasielastic radiative tails, so the integral over two photon phase space can be calculated straightforwardly (using Monte Carlo methods, for example). The corresponding corrections will be considered elsewhere.

Now new methods of experimental data processing, when experimental information about spin observables is extracted directly from polarized parts of cross sections (difference of observed cross sections with opposite spin configurations) [58], are actively developing. It makes new requirements for an accuracy of radiative correction calculations. We note that there is no any cancellation of leading contributions in this case, and factorizing terms in (1.3.28) give the basic contribution.

From the other hand, our result can be used as a contribution to the first order radiative correction to radiative polarized DIS, when radiated photon is tagged in calorimeter. Radiative events cover a much wider region of kinematical variables, so the detection of hard photons, for example, in deep inelastic scattering can provide additional physical information [41, 59] about structure functions in the region unreachable in current experiments. Note that radiative events are used also for luminosity measurements in experiments at HERA.

There is one particular phenomenon. Note, that $P_{\rho\sigma}^{(1)}$ contains not only the imaginary part, but also a certain real part, which comes from the imaginary parts of A_1 and B_1. The multiplication of this real part of $P_{\rho\sigma}^{(1)}$ with the ordinary symmetrical part of the hadronic tensor will give rise to a one-spin azimuthal asymmetry for the final electron [60]. The asymmetry is proportional to the degree of polarization of the initial electron. It is small (few percent) because of the extra power of α_{QED} and the absence of large logarithms.

Here we considered the typical kinematical case when the photon can be resolved. The kinematical situation when photon is emitted close to initial or the scattered electron directions was considered in paper [61].

1.4. Hadronic Cross Sections in Electron-Positron Annihilation with Tagged Photon. Let us consider now the cross channel to DIS with hard photon tagging process — the initial state radiation of hard photon in the single virtual high-energy e^+e^--pair annihilation into hadrons [62].

1.4.1. Introduction. Experiments with tagged photons, radiated from the initial state in electron–proton and electron–positron collisions, can become particularly attractive. The reason is that these radiative processes will permit one to extract information about the final states at continuously varying values of the collision energy. To investigate deep inelastic scattering the authors of Ref. 41 suggested to use radiative events instead of running colliders at reduced beam energies. The method takes advantage of a photon detector (PD) placed in the very forward direction, as seen from the incoming electron beam. The effective beam energy, for each radiative event, is determined by the energy of the hard photon observed in PD. In fact, radiative events were already used to measure the structure function F_2 down to $Q^2 \geq 1.5$ GeV^2 [36, 63]. The specific theoretical work concerns the evaluation of QED radiative corrections (see Secs. 1,2) to the radiative Born cross section. With an accurate determination of the cross sections

and of the possible sources of background we believe that the use of radiative events may become particularly useful to carry investigations at various present and future machines.

The important role of the initial state radiation in the process of electron–positron annihilation was underlined in a series of papers by V.N. Baier and V.A. Khoze [64], where the radiative process was studied in detail in the Born approximation. In these papers the mechanism of returning to a resonant region was discovered. This mechanism consists in the preferable emission of photons from the initial particles, which provides a resonant kinematics of a subprocess. A utilization of radiative events can become a common type of investigations at various machines.

In this part we derive explicit formulae for the spectrum of tagged photons. The calculations are performed having an accuracy of the per-mille order as an aim. Formulae can be used at electron–positron colliders to investigate, for instance, hadronic final states at intermediate energies. A measurement of the total hadronic cross section at low energies is essential for high precision test of the Standard Model particularly for a precise determination of the fine structure constant $\alpha_{\mathrm{QED}}(M_Z)$ and of the muon anomalous magnetic moment $(g-2)_\mu$. The largest contribution to the errors for these quantities comes from the large indetermination still present on the measurement of the total hadronic cross section in electron–positron annihilation at the centre-of-mass energies of a few GeV. We will consider here the radiatively corrected cross section for the electron–positron annihilation process

$$e^-(p_1) \; + \; e^+(p_2) \; \longrightarrow \; \gamma(k) \; + \; H(q), \qquad k = (1-z)p_1, \qquad (1.4.1)$$

where H is a generic hadronic state. The hard photon hitting the photon detector has a momentum k and an energy fraction $1-z$ with respect to the beam energy. In the following we assume that the photon detector is placed along the electron beam direction, and has an opening angle $2\theta_0 \ll 1$, such that $\varepsilon^2\theta_0^2 \gg m^2$, with m the electron mass, and ε the beam energy. To evaluate the process with an accuracy of the per mille requires a careful investigation of the radiative corrections. This part is organized as follows. In Section 1.4.2 we consider the cross section of the process (1.4.1) in the Born approximation. We give formulae suitable to study as differential distributions in hadronic channels, as well as the total (in terms of quantity R) and inclusive (in terms of hadron fragmentation functions) hadronic cross sections. In Sec. 1.4.3 we calculate separate contributions into radiatively corrected cross section of process (1.4.1) within the next–to–leading accuracy. In Sec. 1.4.3.1 the contribution due to virtual and soft photon emission is investigated. In Sec. 1.4.3.2 the case, when additional hard photon hits a photon detector is considered. In Sec. 1.4.3.3 the contribution due to hard photon emission, which does not hit a photon detector, is derived. In Sec. 1.4.4 we sum

up all the contributions and give the final result. In Conclusion we summarize the results and give some numerical illustrations.

1.4.2. The Born Approximation. In order to obtain the Born approximation for the cross section of the process (1.4.1), when the PD is placed in front of electron (positron) beam, we can use the quasireal electron method [49]. It gives

$$d\sigma(k, p_1, p_2) = dW_{p_1}(k)\sigma_0(p_1 - k, p_2), \tag{1.4.2}$$

where $dW_{p_1}(k)$ is the probability to radiate photon with energy fraction $1 - z$ inside a narrow cone with the polar angle not exceeding $\theta_0 \ll 1$ around the incoming electron, and $d\sigma_0$ is the differential cross section for the radiationless process of electron–positron annihilation into hadrons at the reduced electron beam energy. The form of both, $dW_{p_1}(k)$ and $\sigma_0(p_1 - k, p_2)$ is well known:

$$dW_{p_1}(k) = \frac{\alpha}{2\pi} P_1(z, L_0) dz, \quad P_1(z, L_0) = \frac{1 + z^2}{1 - z} L_0 - \frac{2z}{1 - z},$$
$$L_0 = \ln \frac{\varepsilon^2 \theta_0^2}{m^2}. \tag{1.4.3}$$

We need further the general form of the lowest order cross section σ_0 for the process $e^+(z_1 p_2) + e^-(z p_1) \rightarrow$ hadrons boosted along the beam axis ($\boldsymbol{p}_1$):

$$\sigma_0(z, z_1) = \frac{8\pi^2 \alpha^2}{q^2 |1 - \Pi(q^2)|^2} \int T(q) d\Gamma(q), \qquad T(q) = \frac{L_{\rho\sigma} H_{\rho\sigma}}{(q^2)^2}, \tag{1.4.4}$$

$$L_{\rho\sigma} = \frac{q^2}{2} \widetilde{g}_{\rho\sigma} + 2z^2 \widetilde{p}_{1\rho} \widetilde{p}_{1\sigma}, \quad d\Gamma(q) = (2\pi)^4 \delta(q - \sum q_j) \prod \frac{d^3 q_j}{2\varepsilon_j (2\pi)^3},$$

$$q = zp_1 + z_1 p_2, \qquad q^2 = sz_1 z,$$

$$\widetilde{g}_{\rho\sigma} = g_{\rho\sigma} - \frac{q_\rho q_\sigma}{q^2}, \qquad \widetilde{p}_{1\rho} = p_{1\rho} - \frac{p_1 q}{q^2} q_\rho, \tag{1.4.5}$$

where q is the full 4-momentum of final hadrons, q_j is 4-momentum of an individual hadron, $s = 2p_1 p_2 = 4\varepsilon^2$ is the full centre-of-mass energy squared, and $H_{\rho\sigma}$ is the hadronic tensor. The vacuum polarization operator $\Pi(q^2)$ of the virtual photon with momentum q is a known function [65] and will not be specified here.

The tensors $H_{\rho\sigma}$ and $L_{\rho\sigma}$ obey the current conservation conditions once saturated with the 4-vector q. The differential cross section with respect to the tagged photon energy fraction z can be obtained by performing the integration on the hadrons phase space. It takes the form

$$\frac{d\sigma}{dz} = \frac{\alpha}{2\pi} P_1(z, L_0) \, \sigma_0(z, 1). \tag{1.4.6}$$

Each hadronic state is described by its own hadronic tensor. The cross section in Eqs. (1.4.2) and (1.4.4) is suitable for different uses and, as mentioned above, it can be used to check different theoretical predictions.

The sum of the contributions of all hadronic channels by means of the relation

$$\sum_h \int H_{\rho\sigma} \mathrm{d}\Gamma = f_h(q^2)\widetilde{g}_{\rho\sigma}\,, \tag{1.4.7}$$

can be expressed in terms of the ratio of the total cross section for annihilation into hadrons and muons $R = \sigma_h/\sigma_\mu$. For the $\mu^+\mu^-$ final state we get

$$f_\mu = \frac{q^2}{6\pi}K(q^2), \qquad K(q^2) = \left(1 + \frac{2m_\mu^2}{q^2}\right)\sqrt{1 - \frac{4m_\mu^2}{q^2}},$$

and so,

$$f_h(q^2) = \frac{q^2 R(q^2)}{6\pi}K(q^2). \tag{1.4.8}$$

Substituting this expression into the right-hand side of Eqs. (1.4.2) and (1.4.4) results in the replacement $\sigma_0(z, z_1) = R(q^2)4\pi\alpha^2 K(q^2)/(3q^2)$.

In experiments of semiinclusive type one fixes an hadron with 3-momentum q_1, energy ε_1 and mass M in every event and sum over all the rest. In this case instead of Eq. (1.4.7) we will have (similarly to the Deep Inelastic Scattering (DIS) case [51, 52, 66]):

$$\sum_{h'} \int H_{\rho\sigma} \mathrm{d}\Gamma = H_{\rho\sigma}^{(1)} \frac{\mathrm{d}^3 q_1}{2\varepsilon_1(2\pi)^3}\,,$$

$$H_{\rho\sigma}^{(1)} = F_1(\eta, q^2)\widetilde{g}_{\rho\sigma} - \frac{4}{q^2}F_2(\eta, q^2)\widetilde{q}_{1\rho}\widetilde{q}_{1\rho}, \quad \eta = \frac{q^2}{2qq_1} > 1\,, \tag{1.4.9}$$

where we have introduced two dimentionless functions $F_1(\eta, q^2)$ and $F_2(\eta, q^2)$ in a way similar to the DIS case.

By introducing the dimentionless variable $\lambda = 2qq_1/(2zp_1q_1)$, we can write the corresponding cross section for radiative events in e^+e^- annihilation in the same form as in the case of deep inelastic scattering with a tagged photon [51, 52, 66]:

$$\frac{\mathrm{d}\sigma}{\mathrm{d}z} = \frac{\alpha^2(q^2)}{2\pi}\frac{\alpha}{2\pi}P_1(z, L_0)\Sigma(\eta, \lambda, q^2)\frac{1}{(q^2)^2}\frac{\mathrm{d}^3 q_1}{\varepsilon_1}\,,$$

$$\Sigma(\eta, \lambda, q^2) = F_1(\eta, q^2) + \frac{2F_2(\eta, q^2)}{\eta^2\lambda^2}\left(\lambda - 1 - \frac{M^2}{q^2}\eta^2\lambda^2\right). \tag{1.4.10}$$

1.4.3. Radiative Corrections. For the radiative corrections (RC) to the cross section (1.4.6) we will restrict ourselves only to terms containing second and first powers of large logarithms L, and omit terms which don't contain them, i.e., we will keep leading and next-to-leading logarithmic contributions. We will consider in Section 3.1 the contribution from one-loop virtual photon as well as from the emission of soft real ones. In 3.2 we will discuss the double hard photon emission process.

1.4.3.1. Corrections Due to Virtual and Real Soft Photons. The interference of Born and one–loop contributions to the amplitude of the initial state radiation in annihilation of e^+e^- into hadrons can be obtained from the analogous quantity of hard photon emission in electron–proton scattering [51, 52, 66]. We do that by using the crossing transformation. For the contribution coming from the emission of real soft photons a straightforward calculation gives:

$$\frac{d\sigma^S}{d\sigma_0} = \frac{\alpha}{\pi}\left[2(L_s - 1)\ln\frac{m\Delta\varepsilon}{\lambda\varepsilon} + \frac{1}{2}L_s^2 - \frac{\pi^2}{3}\right],$$

$$L_s = \ln\frac{s}{m^2} = L_0 + L_\theta, \qquad L_\theta = \ln\frac{4}{\theta^2}, \qquad (1.4.11)$$

where λ is the *photon mass*, $\Delta\varepsilon$ is the energy carried by the soft photon. The sum of the two contributions is free from infrared singularities. It reads

$$d\sigma^{V+S} = \frac{8\pi^2\alpha^2}{s|1-\Pi(q^2)|^2}\frac{\alpha}{2\pi}[\rho B_{\rho\sigma}(q) + A_{\rho\sigma}(q)]\frac{H_{\rho\sigma}(q)d\Gamma(q)}{(q^2)^2}\frac{\alpha}{4\pi^2}\frac{d^3k}{\omega}, \tag{1.4.12}$$

where

$$\rho = 4(L_s - 1)\ln\Delta + 3L_q - \frac{\pi^2}{3} - \frac{9}{2}, \quad L_q = L_s + \ln z, \quad \Delta = \frac{\Delta\varepsilon}{\varepsilon} \ll 1, \tag{1.4.13}$$

where k and ω are the 3-momentum and the energy of the hard photon respectively. The tensors $A_{\rho\sigma}$ and $B_{\rho\sigma}$ have a rather involved form. The first can be obtained from the corresponding expressions of Refs. 13, 33. The tensor $B_{\rho\sigma}$ coincides with the one of the Born approximation. In the kinematical region where the hard photon is emitted close to the initial electron direction of motion one has

$$B_{\rho\sigma} = \frac{2}{z}\left(\frac{1+z^2}{y_1(1-z)} - \frac{2m^2z}{y_1^2}\right)L_{\rho\sigma}(q), \quad A_{\rho\sigma} = \frac{2}{q^2}A_g L_{\rho\sigma}(q), \quad q = zp_1 + p_2, \tag{1.4.14}$$

where tensor $L_{\rho\sigma}$ is given in Eq. (1.4.4), $y_1 = 2kp_1$, and quantity A_g reads

$$
A_g = \frac{4zsm^2}{y_1^2} L_s \ln z + \frac{s}{y_1}\left[\frac{1+z^2}{1-z}(-2L_s \ln z - \ln^2 z + 2\mathrm{Li}_2(1-z)+\right.
$$

$$
\left.+2\ln\frac{y_1}{m^2}\ln z) + \frac{1+2z-z^2}{2(1-z)}\right], \qquad \mathrm{Li}_2(x) = -\int_0^1 \mathrm{d}t\frac{\ln(1-tx)}{t}. \quad (1.4.15)
$$

Further integration over the hard photon phase space can be performed within the logarithmic accuracy by using the integrals

$$
\int \frac{\mathrm{d}^3 k}{2\pi k_0}\left[\frac{1}{y_1}, \frac{m^2}{y_1^2}, \frac{\ln(y_1/m^2)}{y_1}\right] = \left[\frac{1}{2}L_0, \frac{1}{2(1-z)}, \frac{1}{4}L_0^2 + \frac{1}{2}L_0\ln(1-z)\right]\mathrm{d}z.
$$

The final expression for the Born cross section corrected for the emission of soft and virtual photons has the form

$$
\frac{\mathrm{d}\sigma^{B+V+S}}{\mathrm{d}z} = \sigma_0(z,1)\left[\frac{\alpha}{2\pi}P_1(z,L_0) + \left(\frac{\alpha}{2\pi}\right)^2(\rho P_1(z,L_0) + N)\right],
$$

$$
N = -\frac{1+z^2}{1-z}\left[(L_0 + \ln z)\ln z - \frac{\pi^2}{3} + 2\mathrm{Li}_2(z)\right]L_0 - 2P_1(z,L_0)\ln\frac{\theta_0^2}{4}+
$$

$$
+\frac{1+2z-z^2}{2(1-z)}L_0 + \frac{4z}{1-z}L_0\ln z. \qquad (1.4.16)
$$

1.4.3.2. Two Hard Photons Tagged by the Detector. If an additional hard photon emitted by the initial-state electron hits the PD, we cannot use the quasireal electron method and have to calculate the corresponding contribution starting from Feynman diagrams.

We can use double hard photon spectra as given in Ref. 67 for annihilation diagrams only and write the cross section under consideration as follows

$$
\frac{\mathrm{d}\sigma_{c1}^H}{\mathrm{d}z} = \sigma_0(z,1)\left(\frac{\alpha}{2\pi}\right)^2 L_0 \int\limits_\Delta^{1-z-\Delta}\frac{\mathrm{d}x}{\xi}\left[\frac{\gamma\tau}{2}L_0 + (z^2 + (1-x)^4)\times\right.
$$

$$
\left.\times\ln\frac{(1-x)^2(1-z-x)}{zx} + zx(1-z-x) - x^2(1-x-z)^2 - 2\tau(1-x)\right],
$$

$$
\xi = x(1-x)^2(1-z-x), \quad \gamma = 1 + (1-x)^2, \quad \tau = z^2 + (1-x)^2. \quad (1.4.17)
$$

Here the variable x under the integral sign is the energy fraction of one hard photon. The quantity $1 - z - x$ is the energy fraction of the second hard photon provided that their total energy fraction equals $1 - z$. We write the index $c1$ in the left-hand side of Eq. (1.4.3) to emphasize that this contribution arises from the collinear kinematics, when the additional hard photon is emitted along the initial electron with 4-momentum p_1.

The integration in the right-hand side of Eq. (1.4.3) leads to the result

$$
\frac{\mathrm{d}\sigma_{c1}^H}{\mathrm{d}z} = \sigma_0(z,1)\left(\frac{\alpha}{2\pi}\right)^2 \frac{L_0}{2}\left\{\left[P_\Theta^{(2)}(z) + 2\frac{1+z^2}{1-z}\left(\ln z - \frac{3}{2} - 2\ln\Delta\right)\right]L_0 + \right.
$$

$$
\left. + \quad 6(1-z) + \frac{3+z^2}{1-z}\ln^2 z - \frac{4(1+z)^2}{1-z}\ln\frac{1-z}{\Delta}\right\}, \tag{1.4.18}
$$

where the quantity $P_\Theta^{(2)}(z)$ represents the so-called Θ term of the second-order electron structure function:

$$
P_\Theta^{(2)}(z) = 2\frac{1+z^2}{1-z}\left(\ln\frac{(1-z)^2}{z} + \frac{3}{2}\right) + (1+z)\ln z - 2(1-z). \tag{1.4.19}
$$

1.4.3.3. Additional Hard Photon Emitted Outside PD. If an additional hard photon, emitted from the initial state, does not hit the PD situated in the direction of motion of the initial electron we distinguish the case when it is emitted in the direction close, within a small cone with angle $\theta' \ll 1$, to the direction of the initial positron. In this case we obtain:

$$
\frac{\mathrm{d}\sigma_{c2}^H}{\mathrm{d}z} = \frac{\alpha}{2\pi}P_1(z,L_0)\int_\Delta^{1-\delta/z}\frac{\alpha}{2\pi}P_1(1-x,L')\sigma_0(z,1-x)\mathrm{d}x, \tag{1.4.20}
$$

where $L' = L_s + \ln(\theta'^2/4)$, $\delta = M^2/s$, and M^2 is the minimal hadron mass squared. We suppose that $z \sim 1$.

We have introduced the additional auxiliary parameter $\theta' \ll 1$ which, together with θ_0, separates collinear and semicollinear kinematics of the second hard photon. Contrary to θ_0, which is supposed to determine the PD acceptance, θ' will disappear in the sum of the collinear and semicollinear contributions of the

second photon. This last kinematical region gives

$$
\frac{\mathrm{d}\sigma_{sc}^H}{\mathrm{d}z} = \left(\frac{\alpha}{2\pi}\right)^2 P_1(z, L_0) \int \frac{\mathrm{d}^3 k_1}{2\pi\omega_1^3} \frac{16\pi^2\alpha^2}{(1-c^2)z^2} T(c, z, x),
$$

$$
T(c, z, x) = \int \frac{H_{\rho\sigma}(q_2)\mathrm{d}\Gamma(q_2)}{s(q_2^2)^2|1 - \Pi(q_2^2)|^2} \left[\frac{s}{2}((z - x_2)^2 + z^2(1 - x_1)^2)g_{\rho\sigma} + \right.
$$

$$
+ \left. 2(z(1 - x_1) - x_2)(z^2 p_{1\rho}p_{1\sigma} + p_{2\rho}p_{2\sigma})\right],
$$

$$
x_1 = \frac{x}{2}(1 - c), \qquad x_2 = \frac{x}{2}(1 + c),
$$

$$
q_2 = zp_1 + p_2 - k_1, \qquad c = \cos\widehat{k_1 p_1}. \tag{1.4.21}
$$

The phase volume of the second photon is parametrized as:

$$
\int \frac{\mathrm{d}^3 k_1}{2\pi\omega^3} = \int\limits_{\Delta}^{\hat{x}} \frac{\mathrm{d}x}{x} \int\limits_0^{2\pi} \frac{\mathrm{d}\phi}{2\pi} \int\limits_{-1+\theta'^2/2}^{1-\theta_0^2/2} \mathrm{d}c, \qquad \hat{x} = \frac{2(z - \delta)}{1 + z + c(1 - z)}. \tag{1.4.22}
$$

Explicitly extracting the angular singularities we represent this expression as

$$
\frac{\mathrm{d}\sigma_{sc}^H}{\mathrm{d}z} = \left(\frac{\alpha}{2\pi}\right)^2 P_1(z, L_0)\left[\Sigma_{sc}(z) + \ln\frac{4}{\theta_0^2} \int\limits_{\Delta}^{z-\delta} \frac{\mathrm{d}x}{x} \frac{z^2 + (z - x)^2}{z^2} \times \right.
$$

$$
\times \sigma_0(z - x, 1) + \ln\frac{4}{\theta'^2} \int\limits_{\Delta}^{1-\delta/z} \frac{\mathrm{d}x}{x}(1 + (1 - x)^2)\sigma_0(z, 1 - x)\right], \tag{1.4.23}
$$

$$
\Sigma_{sc} = \frac{8\pi^2\alpha^2}{z^2} \int\limits_{-1}^1 \mathrm{d}c \int\limits_{\Delta}^{\hat{x}} \frac{\mathrm{d}x}{x}\left[\frac{T(c, z, x) - T(1, z, x)}{1 - c} + \frac{T(c, z, x) - T(-1, z, x)}{1 + c}\right].
$$

1.4.4.4. Complete QED Correction and Leading Logarithmic Approximation. The final result in the order $\mathcal{O}(\alpha)$ for radiative corrections

to radiative events can be written as follows:

$$\frac{d\sigma}{dz} = \frac{\alpha}{2\pi}P_1(z, L_0)\sigma_0(z, 1)(1 + r) = \frac{\alpha}{2\pi}P_1(z, L_0)\sigma_0(z, 1) + \left(\frac{\alpha}{2\pi}\right)^2 \times$$

$$\times \left\{ L_0\left(\frac{1}{2}L_0 P^{(2)}(z) + G\right)\sigma_0(z, 1) + P_1(z, L_0)\left[\int_0^{1-\delta/z} C_1(x)\sigma_0(z, 1 - x)dx + \right.\right.$$

$$\left.\left. + L_\theta \int_0^{z-\delta} C_2(z, x)\sigma_0(z - x, 1)dx + \Sigma_{sc}\right]\right\}, \tag{1.4.24}$$

where the last term is defined by Eq. (1.4.3) and

$$C_1(x) = P_1(1 - x, L_s)\Theta(x - \Delta) + (L_s - 1)(2\ln\Delta + \frac{3}{2})\delta(x),$$

$$C_2(z, x) = \frac{z^2 + (z - x)^2}{z^2 x}\Theta(x - \Delta) + (2\ln\Delta + \frac{3}{2} - 2\ln z)\delta(x),$$

$$G(z) = \frac{1 + z^2}{1 - z}(3\ln z - 2\text{Li}_2(z)) + \frac{1}{2}(1 + z)\ln^2 z -$$

$$- \frac{2(1 + z)^2}{1 - z}\ln(1 - z) + \frac{1 - 16z - z^2}{2(1 - z)} + \frac{4z\ln z}{1 - z}. \tag{1.4.25}$$

In order to include the higher order leading corrections to the tagged photon differential cross section and to show the agreement of our calculation with the well-known Drell–Yan representation for the total hadronic cross section at electron–positron annihilation [31]

$$\sigma(s) = \int_\delta^1 dx_1 \int_{\delta/x_1}^1 dx_2 \, D(x_1, \alpha_{\text{eff}})D(x_2, \alpha_{\text{eff}})\sigma(x_1 x_2 s), \tag{1.4.26}$$

where the electron structure functions include both nonsinglet and singlet parts

$$D(x_1, \alpha_{\text{eff}}) = D^{NS}(x, \alpha_{\text{eff}}) + D^S(x_1, \alpha_{\text{eff}}), \tag{1.4.27}$$

it is convenient to introduce the quantity

$$\Sigma = D(z, \bar{\alpha}_{\text{eff}}) \int_{\delta/z}^1 dx_1 \int_{\delta/zx_1}^1 dx_2 \, D(x_1, \widetilde{\alpha}_{\text{eff}})D(x_2, \hat{\alpha}_{\text{eff}})\sigma_0(zx_1, x_2). \tag{1.4.28}$$

Note that the shifted cross section in Eq. (1.4.26) has just the same meaning as in Eq. (1.4.4): $\sigma(x_1 x_2 s) = \sigma_0(x_1, x_2)$.

The structure functions [68, 69] entering RHS of Eq. (1.4.27) are

$$D^{NS}(x, \alpha_{\text{eff}}) = \delta(1 - x) + \sum_{n=1}^{\infty} \frac{1}{n!} \left(\frac{\alpha_{\text{eff}}}{2\pi} \right)^n P_1^{\otimes n}(x), \qquad (1.4.29)$$

$$D^S(x, \alpha_{\text{eff}}) = \frac{1}{2!} \left(\frac{\alpha_{\text{eff}}}{2\pi} \right)^2 R(x) + \frac{1}{3!} \left(\frac{\alpha_{\text{eff}}}{2\pi} \right)^3 \left[2P_1 \otimes R(x) - \frac{2}{3} R(x) \right],$$
$$(1.4.30)$$

where

$$
\begin{aligned}
P_1(x) &= \lim_{\Delta \to 0} \left\{ \frac{1 + x^2}{1 - x} \Theta(1 - \Delta - x) + \left(\frac{3}{2} + 2 \ln \Delta \right) \delta(1 - x) \right\}, \\
R(x) &= 2(1 + x) \ln x + \frac{1 - x}{3x}(4 + 7x + 4x^2), \\
P_1^{\otimes n} &= \underbrace{P_1(x) \otimes \cdots \otimes P_1(x)}_{n}, \qquad P_1(x) \otimes P_1(x) = \int_x^1 P_1(t) P_1\left(\frac{x}{t} \right) \frac{\mathrm{d}t}{t},
\end{aligned}
$$

and the effective electromagnetic couplings in the RHS of Eq. (1.4.28) are

$$
\begin{aligned}
\bar{\alpha}_{\text{eff}} &= -3\pi \ln\left(1 - \frac{\alpha}{3\pi} L_0 \right), \\
\widetilde{\alpha}_{\text{eff}} &= -3\pi \ln\left(\frac{1 - \frac{\alpha}{3\pi} L_s}{1 - \frac{\alpha}{3\pi} L_0} \right), \\
\hat{\alpha}_{\text{eff}} &= -3\pi \ln\left(1 - \frac{\alpha}{3\pi} L_s \right). \qquad (1.4.31)
\end{aligned}
$$

At fixed values of z ($z < 1$) the quantity Σ defines the leading logarithmic contributions into differential cross section for the events with tagged particles. That corresponds to only Θ terms in the expansion of the structure function $D(z, \bar{\alpha}_{\text{eff}})$ before the integral sign in Eq. (1.4.28). If we consider photonic corrections (as do in the previous sections), it is needed to restrict ourselves to the nonsinglet part of the electron structure functions and with the first order terms in the expansion of all effective couplings, namely:

$$\bar{\alpha}_{\text{eff}} \to \alpha L_0, \quad \widetilde{\alpha}_{\text{eff}} \to \alpha L_\theta, \quad \hat{\alpha}_{\text{eff}} \to \alpha L_s. \qquad (1.4.32)$$

It is easy to see that in this case the leading contribution into differential cross section (1.4.3) can be obtained as an expansion of the quantity $\Sigma(z < 1)$ by the powers of α, keeping the terms of the order α^2 in the production of D functions.

If we want to include the contribution due to e^+e^--pair (real and virtual) production it is required [70] to use both nonsinglet and singlet structure functions and effective couplings defined by Eq. (1.4.31). Note that the insertion into consideration of higher order corrections rises additional questions about concrete experimental conditions concerning registration of events with e^+e^- pairs.

The total hadronic cross section in e^+e^- annihilation can be obtained by integration of quantity Σ over z

$$\sigma(s) = \int\limits_{\delta}^{1} dz \, D(z, \bar{\alpha}_{\text{eff}}) \int\limits_{\delta/z}^{1} dx_1 \int\limits_{\delta/zx_1}^{1} dx_2 \, D(x_1, \widetilde{\alpha}_{\text{eff}}) D(x_2, \hat{\alpha}_{\text{eff}}) \sigma(zx_1x_2s).$$

(1.4.33)

We can integrate the expression in the right side of Eq. (1.4.33) over the variable z provided the quantity $zx_1 = y$ is fixed

$$\int\limits_{\delta}^{1} dz \, D(z, \bar{\alpha}_{\text{eff}}) \int\limits_{\delta/z}^{1} dx_1 \, D(x_1, \widetilde{\alpha}_{\text{eff}}) = \int\limits_{\delta}^{1} dz \int\limits_{y}^{1} dy \, D(z, \bar{\alpha}_{\text{eff}}) \times$$

$$\times D\left(\frac{y}{z}, \widetilde{\alpha}_{\text{eff}}\right) = \int\limits_{\delta}^{1} dy \, D(y, \bar{\alpha}_{\text{eff}} + \widetilde{\alpha}_{\text{eff}}), \quad \bar{\alpha}_{\text{eff}} + \widetilde{\alpha}_{\text{eff}} = \hat{\alpha}_{\text{eff}}.$$

(1.4.34)

Using this result and definition of $\hat{\alpha}_{\text{eff}}$ we indicate the equivalence of the Drell–Yan form of the total cross section as given by Eq. (1.4.26) and the representation of the cross section by Eq. (1.4.33).

Let us show now that D functions in expression for the quantity Σ have effective couplings as given by Eq. (1.4.31). By definition the nonsinglet electron structure function satisfies the equation [71]

$$D(x, s, s_0) = \delta(1 - x) + \frac{1}{2\pi} \int\limits_{s_0}^{s} \frac{ds_1}{s_1} \alpha(s_1) \int\limits_{x}^{1} \frac{dz}{z} D(z) D\left(\frac{x}{z}, \frac{s_1}{s_0}\right), \quad (1.4.35)$$

where $\alpha(s_1)$ is the electromagnetic running coupling

$$\alpha(s_1) = \alpha\left(1 - \frac{\alpha}{3\pi} \ln \frac{s_1}{m^2}\right)^{-1},$$

and $s_0(s)$ is the minimal (maximal) virtuality of the particle, which radiates photons and e^+e^- pairs.

The structure function $D(z, \bar{\alpha}_{\text{eff}})$ describes the photon emission and pair production inside narrow cone along the electron beam direction. In this kinematics $s_0 = m^2$, $s = \varepsilon^2 \theta_0^2$. The corresponding iterative solution of Eq. (1.4.35) has the form (1.4.29) with $\alpha_{\text{eff}} = \bar{\alpha}_{\text{eff}}$. The structure function $D(x_1, \widetilde{\alpha}_{\text{eff}})$ describes the events, when emitted (by the electron) particles escape this narrow cone. In this case $s_0 = \varepsilon^2 \theta_0^2$, $s = 4\varepsilon^2$. The corresponding solution of Eq. (1.4.35) gives the structure function with $\alpha_{\text{eff}} = \widetilde{\alpha}_{\text{eff}}$. At last, the structure function $D(x_2, \hat{\alpha}_{\text{eff}})$ is responsible for the radiation off the positron into the whole phase space. In this case $s_0 = m^2$, $s = 4\varepsilon^2$. Therefore we obtain D function with $\alpha_{\text{eff}} = \hat{\alpha}_{\text{eff}}$. The analogous consideration can be performed for the singlet part of structure functions.

When writing the representation (1.4.33) for the total cross section we, in fact, divide the phase space of the particles emitted by the electron on the regions inside and outside the narrow cone along electron beam direction. Therefore we can use this representation to investigate the events with tagged particles in both these regions. As we saw before the differential cross section for events with tagged particles inside the narrow cone is defined by the quantity $\Sigma(z < 1)$. In order to obtain the corresponding differential cross section for events with tagged particles outside this narrow cone we have to change the places of $\bar{\alpha}_{\text{eff}}$ and $\widetilde{\alpha}_{\text{eff}}$ in expression for $\Sigma(z, 1)$. This follows from the symmetry of representation (1.4.33) relative such change.

1.4.4. Conclusion. In sum, the formulae (1.4.34),(1.4.28) are the main results of this part.

Thus we calculated the cross section of e^+e^- annihilation with detection of a hard photon at small angles with respect to the electron beam. The general structure of a measured cross section, from which one should extract the annihilation cross section σ_0, looks

$$\sigma = \sigma_0 \left[a_1 \frac{\alpha}{\pi} L + b_1 \frac{\alpha}{\pi} + a_2 \left(\frac{\alpha}{\pi} \right)^2 L^2 + b_2 \left(\frac{\alpha}{\pi} \right)^2 L + c_2 \left(\frac{\alpha}{\pi} \right)^2 \right] + \mathcal{O}(\alpha^3),$$

(1.4.36)

where L denotes some large logarithm. We calculated the terms a_1, b_1, a_2, b_2 and some contributions to c_2. The generalized formula (1.4.28) allows one to involve the leading terms of the order $\mathcal{O}(\alpha^3 L^3)$. In this way our formulae provide high theoretical precision.

Similar formulae can be obtained for an experimental set-up by tagging a definite hadron. By using e^+e^- machines such as BEPS, DAΦNE [72], VEPP, CLEO, SLAC–B/factory and others with luminosities of order $10^{33}\, \text{cm}^2 \cdot \text{s}^{-1}$, one is in principle able to scan, by measuring the initial state radiation spectrum,

the whole energy region of hadron production with an effective luminosity of the order of $10^{31}\,\mathrm{cm}^2\cdot\mathrm{s}^{-1}$. Let's hope that further study would be pursuing on these issues from experimental as well as from theoretical point of view.

2. OUTLOOK

Results given in Sections 1.1 and 1.3 could be applied to elastic and quasi-elastic scattering off nuclei. Among possible there are channels with nuclei got excited or even broken apart.

At the moment a tagged photon set-up in DIS as well as annihilation channels (Sections 1.2, 1.4) are of some perspective to high-energy physics in testing QED (SM) predictions for effects induced by virtual corrections. The formulae given here guarantee the theoretical error to fall down to 0.1%.

We did not touch the problem of evaluation of Z, W bosons contribution, which was considered elsewhere, as well as that of double-photon exchange between a lepton and nucleon and a real photon emission by a nucleon (nuclei). The latter has not been investigated in detail up to now. An almost thorough numerical analysis of the RC to DIS was given in the papers cited in the introduction. Nevertheless, the results presented in the review could be used to create more advanced MC generators with accounting for RC at 0.1% level of accuracy. To the moment this programme has been carried out only partially.

APPENDIX A. DETAILS OF MATRIX ELEMENT CALCULUS: THE CASE OF SINGLE PHOTON BREMSSTRAHLUNG

Using the Sudakov decomposition of the 4-vectors in the problem

$$
\begin{aligned}
& p_1' = \alpha_1'\tilde{p}_2 + b\tilde{p}_1 + p_{1\perp}', \quad k_1 = \alpha_1\tilde{p}_2 + x_1\tilde{p}_1 + k_{1\perp}, \\
& q = p_2 - p_2' = \alpha_q\tilde{p}_2 + \beta_q\tilde{p}_1 + q_\perp, \\
& p_2' = \alpha_2'\tilde{p}_2 + \beta_2'\tilde{p}_1 + p_{2\perp}', \quad v_\perp p_1 = v_\perp p_2 = 0, \\
& \tilde{p}_1 = p_1 - p_2\frac{m^2}{s}, \quad \tilde{p}_2 = p_2 - p_1\frac{M^2}{s},
\end{aligned} \tag{A.1}
$$

we have excluded parameters $\alpha_1, \alpha_1', \beta_q$ using the on-shell conditions

$$
\begin{aligned}
& p_2'^2 - M^2 = -s\beta_q(1 - \alpha_q) - \mathbf{q}^2 - \alpha_q M^2 = 0, \\
& p_1'^2 = sb\alpha_1' - \mathbf{p}_1'^2 = 0, \quad k_1^2 = sx_1\alpha_1 - \mathbf{k}_1^2 = 0,
\end{aligned} \tag{A.2}
$$

besides

$$\Phi^{\text{prot}} = \frac{1}{s^2} \operatorname{Sp} \{(\hat{p}_2' + M)\Gamma_\rho(\hat{p}_2 + M)\tilde{\Gamma}_\sigma p_1^\rho p_1^\sigma\},$$

$$\Gamma_\rho = F_1(q^2)\gamma_\rho + \frac{\sigma_{\mu\rho}q^\mu}{2M}F_2(q^2). \tag{A.3}$$

Here $F_{1,2}(q^2)$ are the Dirac and Pauli form factors of a proton. For Φ^γ we have:

$$\Phi^\gamma = -\frac{1}{s^2} \operatorname{Sp} \{\hat{p}_1' O_\mu \hat{p}_1 \tilde{O}^\mu\},$$

$$O_\mu = \hat{p}_2 \frac{\hat{p}_1 - \hat{k}_1}{-2p_1 k_1}\gamma_\mu + \gamma_\mu \frac{\hat{p}_1' + \hat{k}_1}{2p_1' k_1}\hat{p}_2, \tag{A.4}$$

and then

$$q^2 = -Q_h^2 = -\frac{1}{1 - \alpha_q}[\mathbf{q}^2 + M^2\alpha_q^2] \approx -[\mathbf{q}^2 + Q_{\text{min}}^2], \tag{A.5}$$

with Q_{min}^2 given in the text. The matrix element

$$M = \frac{1}{q^2}J_\sigma^{(1)}\bar{u}(p_2')\Gamma_\rho u(p_2)g^{\rho\sigma}, \tag{A.6}$$

using the Gribov representation for the metric tensor

$$g^{\rho\sigma} = g_\perp^{\rho\sigma} + \left(\frac{2}{s}\right)(\tilde{p}_2^\rho\tilde{p}_1^\sigma + \tilde{p}_2^\sigma\tilde{p}_1^\rho) \approx \left(\frac{2}{s}\right)\tilde{p}_2^\sigma\tilde{p}_1^\rho, \tag{A.7}$$

may be put in a form

$$M = \frac{2s}{q^2}\left(\frac{1}{s}p_2^\sigma J_\sigma^{(1)}\right)\left(\frac{1}{s}\bar{u}(p_2')\Gamma_\rho u(p_2)p_1^\rho\right). \tag{A.8}$$

Note that each expressions in the parentheses on the r.h.s. of Eq. (A.8) do not depend on s in the limit $s \to \infty$. The expression for Φ^γ may be transformed using the following reduced expression

$$O_\mu = x_1\left[sb\gamma_\mu\left(\frac{1}{n} - \frac{1}{n_1}\right) + \frac{1}{n_1}b\gamma_\mu\hat{q}\hat{p}_2 - \frac{1}{n}\gamma_\mu\hat{p}_2\hat{q}\right],$$

$$x_1 = 1 - b. \tag{A.9}$$

to take the form given in Eq. (1.1.8).

APPENDIX B. DETAILS OF MATRIX ELEMENT CALCULUS: THE CASE OF DOUBLE PHOTON BREMSSTRAHLUNG

Let's first demonstrate that the matrix element of the process

$$\gamma^*(q) + e(p_1) \to e(p_1') + \gamma(k_1) + \gamma(k_2) \tag{B.1}$$

is explicitly proportional to **q** for small values of the latter, which is in fact the requirement of gauge invariance with respect to the virtual photon. The matrix element is described by six diagrams. With regard to the gauge invariance this set can be separated out to the two subsets in each of which the gauge condition is satisfied independently. Introducing the photon-permutating operator $\mathcal{P}_{12}$ we bring the matrix element to the form:

$$\mathcal{M} = (1 + \mathcal{P}_{12})Q, \qquad Q = \mathcal{M}_1 + \mathcal{M}_2 + \mathcal{M}_3, \tag{B.2}$$

where

$$
\begin{aligned}
\mathcal{M}_1 &= \frac{1}{dd_1}\bar{u}(p_1')\hat{p}_2(\hat{p}_1 - \hat{k}_1 - \hat{k}_2 + m) \times \\
&\times \hat{e}_2^*(\hat{p}_1 - \hat{k}_1 + m)\hat{e}_1^* u(p_1), \tag{B.3} \\
\mathcal{M}_2 &= \frac{1}{d_1 d_2'}\bar{u}(p_1')\hat{e}_2^*(\hat{p}_1 - \hat{k}_1 + \hat{q} + m)\hat{p}_2 \times \\
&\times (\hat{p}_1 - \hat{k}_1 + m)\hat{e}_1^* u(p_1), \tag{B.4} \\
\mathcal{M}_3 &= \frac{1}{d' d_2'}\bar{u}(p_1')\hat{e}_2^*(\hat{p}_1 - \hat{k}_1 + \hat{q} + m) \times \\
&\times \hat{e}_1^*(\hat{p}_1 + \hat{q} + m)\hat{p}_2 u(p_1), \tag{B.5}
\end{aligned}
$$

and

$$
\begin{aligned}
d &= d_1 + d_2 - \frac{1}{x_1 x_2}(x_1 \vec{k}_2 - x_2 \vec{k}_1)^2, \\
d' &= d_1' + d_2' + \frac{1}{x_1 x_2}(x_1 \vec{k}_2 - x_2 \vec{k}_1)^2.
\end{aligned}
$$

The permutation operator $\mathcal{P}_{12}$ for the photons acts the following way

$$\mathcal{P}_{12} f(k_1, e_1; k_2, e_2) = f(k_2, e_2; k_1, e_1), \qquad \mathcal{P}_{12}^2 = 1.$$

The quantity Q is gauge invariant regarding the virtual photon k since all permutations of this photon have been taken into account. Therefore Q is proportional to $q_\perp$ in the limit of $q_\perp \to 0$. Indeed, making use of the relations

$$Q = p_{2\mu} Q^\mu, \qquad q_\mu Q^\mu = (\alpha_q \tilde{p}_2 + q_\perp)_\mu Q^\mu = 0, \tag{B.6}$$

we immediately obtain (neglecting the small contribution $\beta_q p_\mu Q^\mu \sim 1/s$)

$$Q = -\frac{q_{\perp\mu}}{\alpha_q} Q^\mu \, . \tag{B.7}$$

Then transform the quantities $\mathcal{M}_j$ to such a form that the noticed low $q_\perp$ behavior is present in their sum Q explicitly. The reason is that in this case all individual large (compared to $q_\perp$) contributions are mutually cancelled. The first step is to use the Dirac equations $\hat{p}_1 u(p_1) = m u_1$, $\bar{u}(p'_1)\hat{p}'_1 = m\bar{u}(p'_1)$ and to rearrange the amplitudes $\mathcal{M}_j$ of Eq. (B.3),

$$\mathcal{M}_1 = \bar{u}(p'_1)\left\{ \frac{s\beta'_1}{d_1}\hat{e}^*_2(\hat{p}_1 - \hat{k}_1 + m)\hat{e}^*_1 - \right.$$

$$\left. - \frac{1}{d_1}\hat{p}_2\hat{q}\hat{e}^*_2(\hat{p}_1 - \hat{k}_1 + m)\hat{e}^*_1 \right\} u(p_1) \, ,$$

$$\mathcal{M}_2 = \bar{u}(p'_1)\left\{ +\frac{s(1-x_1)}{d_1 d'_2}\hat{e}^*_2(\hat{p}_1 - \hat{k}_1 + m)\hat{e}^*_1 - \frac{1}{d'_2}\hat{e}^*_2\hat{p}_2\hat{e}^*_1 + \right.$$

$$\left. + \frac{1}{d_1 d'_2}\hat{e}^*_2\hat{q}\hat{p}_2(\hat{p}_1 - \hat{k}_1 + m)\hat{e}^*_1 \right\} u(p_1) \, , \tag{B.8}$$

$$\mathcal{M}_3 = \bar{u}(p'_1)\left\{ \frac{s}{d' d'_2}\hat{e}^*_2(\hat{p}_1 - \hat{k}_1 + m)\hat{e}^*_1 + \frac{s}{d' d'_2}\hat{e}^*_2\hat{q}\hat{e}^*_1 + \right.$$

$$\left. + \frac{1}{d' d'_2}\hat{e}^*_2(\hat{p}'_1 + \hat{k}_2 + m)\hat{e}^*_1\hat{q}\hat{p}_2 \right\} u(p_1) \, .$$

From these formulae it can be noted that the last terms in $\mathcal{M}_1, \mathcal{M}_2, \mathcal{M}_3$, up to terms of the order of

$$\frac{m^2}{E^2} \, , \quad \theta^2 \, , \quad \frac{m}{E}\theta \, ,$$

are proportional to $q_\perp$,

$$\hat{\tilde{p}}_2 \hat{q} = \hat{\tilde{p}}_2(\alpha_q \hat{\tilde{p}}_2 + \beta_q \hat{p} + \hat{q}_\perp) = \hat{\tilde{p}}_2 \hat{q}_\perp = -\hat{q}\hat{\tilde{p}}_2 \, . \tag{B.9}$$

Next, one can see that the sum of the first three terms in Eqs. (B.8) is also proportional to $q_\perp$ since (for more details see [73])

$$A \equiv \frac{b}{d_1} + \frac{1-x_1}{d_1 d'_2} + \frac{1}{d' d'_2} \, , \qquad A|_{q_\perp \to 0} = 0 \, . \tag{B.10}$$

Finally we consider the sum of the second terms of the quantities $\mathcal{M}_2, \mathcal{M}_3$ given in Eqs. (B.8). Using the relations ([73], Eq.(21)) and

$$(p_1' + k_1 + k_2)^2 = (p_1 - k)^2 = m^2 - \mathbf{k}^2 - s\alpha_k \,,$$

one immediately gets

$$-\frac{\hat{\tilde{p}}_2}{d_2'} + \frac{s(\alpha_q\hat{\tilde{p}}_2 + \hat{q}_\perp)}{d'd_2'} = \frac{s\hat{q}_\perp}{d'd_2'} + \frac{\hat{\tilde{p}}_2\mathbf{q}^2}{d'd_2'} \,. \tag{B.11}$$

Therefore, from Eqs. (B.9), (B.10), (B.11) it is clearly seen that the property illustrated by Eq. (B.7)

$$(\mathcal{M}_1 + \mathcal{M}_2 + \mathcal{M}_3)\,|_{q_\perp \to 0} = 0$$

is evidently satisfied and consequently the quantity $Q = \sum_{j=1}^{3} \mathcal{M}_j$ became a sum of terms explicitly proportional to $q_\perp$,

$$
\begin{aligned}
Q &= \bar{u}(p_1')\bigg\{ As\, \hat{e}_2^*(\hat{p}_1 - \hat{k}_1 + m)\hat{e}_1^* - \\
&\quad - \frac{1}{d_1}\hat{\tilde{p}}_2\hat{q}_\perp\hat{e}_2^*(\hat{p}_1 - \hat{k}_1 + m)\hat{e}_1^* - \\
&\quad - \frac{\mathbf{q}^2}{d'd_2'}\hat{e}_2^*\hat{e}_1^*\hat{\tilde{p}}_2 + \frac{s}{d'd_2'}\hat{e}_2^*\hat{q}_\perp\hat{e}_1^* + \\
&\quad + \frac{1}{d_1 d_2'}\hat{e}_2^*\hat{q}_\perp\hat{\tilde{p}}_2(\hat{p}_1 - \hat{k}_1 + m)\hat{e}_1^* + \\
&\quad + \frac{1}{d'd_2'}\hat{e}_2^*(\hat{p}_1' + \hat{k}_2 + m)\hat{e}_1^*\hat{q}_\perp\hat{\tilde{p}}_2 \bigg\}u(p_1)\,. \tag{B.12}
\end{aligned}
$$

Calculating the contribution of the trace $\mathrm{Sp}\{p_1'Qp_1\tilde{Q}\}$ we neglect masses whose contribution to the quantity $\Phi^{\gamma\gamma}$ may be restored using the general prescription [37]. The corresponding correction has the form:

$$
\begin{aligned}
\Delta_m\Phi^{\gamma\gamma} &= (1 + \mathcal{P}_{12})\bigg\{ -\frac{4m^2}{d_1'^2}\frac{x_2^2 y_1(1 + y_1^2)}{(1 - x_2)^2} \times \\
&\quad \times \frac{\mathbf{q}^2}{(\mathbf{q} - y_1\mathbf{p}_1')^2(\mathbf{q} - \mathbf{p}_1'/b)^2} - \\
&\quad - \frac{4m^2}{d_1^2}\frac{\beta_2^2 z_1(1 + z_1^2)\mathbf{q}^2}{(\mathbf{q} - \mathbf{p}_1')^2(\mathbf{p}_1' - (1 - \beta_2)\mathbf{q})^2} \bigg\}, \tag{B.13}
\end{aligned}
$$

where

$$y_1 = \frac{1 - x_2}{b}, \quad \beta_2 = \frac{x_2}{1 - x_1}, \quad z_1 = \frac{b}{1 - x_1}.$$

APPENDIX C. EVALUATION OF 2-DIMENSIONAL INTEGRALS

The azimuthal integration may be performed making use of the following equality:

$$
\begin{aligned}
J_{12\ldots n} &= \frac{1}{2\pi} \int\limits_0^{2\pi} d\phi \prod_i [a_i + b_i \cos(\phi - \phi_i)]^{-1} = \\
&= \sum_{k=1}^{n} \frac{1}{r_k} \prod_{j \neq k}^{n} \frac{b_k}{b_{kj} + i r_k \sin(\phi_k - \phi_j)},
\end{aligned} \tag{C.1}
$$

with

$$
\begin{aligned}
r_i &= \sqrt{a_i^2 - b_i^2}, \qquad |a_i| > |b_i|, \\
b_{ij} &= b_i a_j - b_j a_i \cos(\phi_i - \phi_j).
\end{aligned}
$$

It is curious to note that the absence of the imaginary part provides an interesting algebraic identity. For $n = 2, n = 3$ it looks

$$
\begin{aligned}
J_{12} &= \frac{1}{d_{12}} \left(\frac{b_1}{r_1} b_{12} + \frac{b_2}{r_2} b_{21} \right), \quad d_{12} = a_{12}^2 - r_1^2 r_2^2, \\
a_{12} &= a_1 a_2 - b_1 b_2 \cos(\phi_1 - \phi_2), \\
J_{123} &= \frac{b_1^2}{r_1} \frac{a_{12} a_{13} - r_1^2 a_{23}}{d_{12} d_{13}} + \frac{b_2^2}{r_2} \frac{a_{21} a_{23} - r_2^2 a_{13}}{d_{12} d_{23}} + \\
&+ \frac{b_3^2}{r_3} \frac{a_{31} a_{32} - r_3^2 a_{12}}{d_{31} d_{32}}.
\end{aligned} \tag{C.2}
$$

This form is convenient for a subsequent integration over $d\mathbf{k}_1^2$.

APPENDIX D. NLO CONTRIBUTIONS FROM VIRTUAL AND SOFT PHOTON EMISSION

To avoid the misprints we use here the notations of the paper [33]

$$
\begin{aligned}
s &= d_1', \quad t = -d_1, \quad u = -Q^2, \\
s + t + u &= q^2, \quad \tilde{f}(s,t) = f(t,s), \quad a = s + t, \\
b &= s + u, \qquad c = u + t.
\end{aligned} \tag{D.1}
$$

The quantities τ_{ij} encountered in the text (see Eq. (1.1.12)) may be written as

$$
\begin{aligned}
\tau_{11} &= -G\left(1+\frac{u^2}{s^2}\right) - \tilde{G}\left(2+\frac{b^2}{t^2}\right) + 2\left[\frac{b^2}{st} + \frac{2u}{a} + \right. \\
&+ \left.\frac{2}{a^2}(u^2-bt)\right]l_{qu} + \frac{b^2}{tc^2}(2c+t)l_{qs} + \frac{2u-s}{s}l_{qt} + \\
&+ \frac{1}{q^2}\left[\frac{4}{a}(bt-u^2) - 4u - 2q^2 + t - \frac{b^2}{c}\right],
\end{aligned}
$$

$$
\begin{aligned}
\tau_{12} &= \frac{c}{s^2}(u-s)G + \frac{1}{t^2}(uq^2-st)\tilde{G} - 2\left[\frac{uq^2}{st} + \frac{2u-s+t}{a} + \right. \\
&+ \left.\frac{2}{a^2}(u^2-cs)\right]l_{qu} + \frac{2c+t}{c^2}\left(s-\frac{u}{t}q^2\right)l_{qs} - \\
&- \frac{c}{bs}(2u-s)l_{qt} + \frac{1}{q^2}\left[\frac{4}{a}(u^2-cs) + 8u + 3t - s + \frac{2}{c}us\right], \quad \text{(D.2)}
\end{aligned}
$$

and the additional notations look

$$
l_{qu} = \ln\frac{q^2}{u}, \quad l_{qs} = \ln\frac{-q^2}{s}, \quad l_{qt} = \ln\frac{q^2}{t}, \quad l_{ut} = \ln\frac{u}{t},
$$

$$
\begin{aligned}
G &= l_{qu}(l_{qt}+l_{ut}) + 2\mathrm{Li}_2\left(1-\frac{t}{q^2}\right) - \\
&- 2\mathrm{Li}_2\left(1-\frac{q^2}{u}\right) - 2\mathrm{Li}_2(1). \quad \text{(D.3)}
\end{aligned}
$$

APPENDIX E. SEMICOLLINEAR KINEMATICS OF PAIR CREATION

The matrix element in the kinematics (1.1.2) may be put in a form (we extract the coupling constant):

$$
M^{(1)} = \frac{1}{q_1^2}J_\nu I_\mu g^{\mu\nu}, \quad J_\nu = \bar{u}(p_-)\gamma_\nu u(p_1), \quad \text{(E.1)}
$$

where the current I describes a pair production by the photon with momentum q_1 off a proton. Using the Sudakov form of the 4-vectors p_- and q with basic 4-vectors p_1 and p_2,

$$
p_- = \alpha_-\tilde{p}_2 + \beta_-\tilde{p}_1 + p_{-\perp}, \quad q = \alpha_q\tilde{p}_2 + \beta_q\tilde{p}_1 + q_\perp,
$$

the representation of the metric tensor

$$
g_{\nu\mu} = g_{\nu\mu\perp} + \frac{2}{s}p_{2\nu}p_{1\mu}
$$

and the gauge condition

$$Iq = I(\beta_q p_1 + q_\perp) = 0, \quad \beta_q + \beta_- = 1,$$

we obtain for the matrix element squared and summed over spin states of electron:

$$\sum |M^{(1)}|^2 = \frac{1}{(q_1^2)^2}\left[-2q_1^2 \mathbf{I}^2 + \frac{8}{\beta_q^2}\left(\mathbf{p}_-\mathbf{I}\right)^2\right]. \tag{E.2}$$

To calculate the quantity $\mathbf{I}^2$, we again present it in the form

$$I = e_{q_1}\mathbf{I} = e_{q_1}^\mu e_q^\nu \frac{2s|\vec{q}|}{q^2 s_1} p_{2\rho} Y_\rho \bar{u}(p_1')O_{\mu\nu}v(p_+),$$

$$s_1 = (p_2 + q_1)^2, \qquad Y_\rho = \bar{u}(p_2)\Gamma_\rho u(p_2'). \tag{E.3}$$

The phase volume is transformed the way to take the following form

$$d\Gamma_4 = (2\pi)^{-8}\frac{1}{8s\beta_-\beta_+ b}d^2q d^2p_- d\beta_-. \tag{E.4}$$

Using

$$\sum |\bar{u}(p_1')O_{\mu\nu}v(p_+)e_{q_1}^\mu e_q^\nu|^2 = 8\left[\frac{b}{\beta_+} + \frac{\beta_+}{b}\right],$$

we obtain the result for the cross section given in the text.

For the kinematics of bremsstrahlung mechanism the matrix element has the form

$$M^{(2)} = \frac{1}{k_1^2}I_\mu J_\nu g^{\mu\nu}, \quad k_1 = p_+ + p_1'. \tag{E.5}$$

Here it is convenient to use alternative basis vectors of Sudakov parameterization

$$p_+ = \alpha_+ q + b_+ \tilde{p}_1' + p_{+\perp}, \quad k_1 = a_1 q + b_1 \tilde{p}_1' + k_{1\perp},$$

$$g_{\mu\nu} = g_{\mu\nu\perp} + \frac{2}{\tilde{s}}q^\nu p_1'^\mu, \quad k_1^2 = \frac{\mathbf{p}_+^2 + m^2 b_1^2}{b_1 - 1} > 0. \tag{E.6}$$

Quite the same manipulations give

$$\sum |M^{(2)}|^2 = 2k_1^2 \mathbf{I}^2 - \frac{8}{b_1^2}\left(\mathbf{k}_1\mathbf{I}\right)^2.$$

Performing the integration over $d^2(p_+)_\perp$ to a logarithmic accuracy and expressing the parameter b_1 in terms of the standard Sudakov decomposition with basic 4-vectors p_1, p_2

$$b_1 = \frac{1 - \beta_-}{b},$$

we immediately obtain the result given in the text.

APPENDIX F

In this section we collect the results of the angular integration of the definite structures of the Compton tensor in [33,46]. Using integrals similarly to (1.2.12) and retaining only terms that contain at least one large logarithm L_0 or L_Q, we obtain

$$
\frac{2\varepsilon^2}{Q_l^2}\int\frac{d\Omega_k}{2\pi}T_g = -\rho\left[\frac{1+z^2}{(1-z)^2}(L_0-1)+1\right]+\frac{1+z^2}{(1-z)^2}[A\ln z+B]-
$$

$$
-\frac{4z}{(1-z)^2}L_Q\ln z-\frac{2-(1-z)^2}{2(1-z)^2}L_0,
$$

$$
2\varepsilon^2\int\frac{d\Omega_k}{2\pi}T_{11} = \frac{4z}{(1-z)^2}\rho L_0-\frac{2z(1+(1-z)^2)}{(1-z)^4}(A\ln z+B)-
$$

$$
-A\frac{z(3-z)}{(1-z)^3}+\frac{2L_0}{(1-z)^3}\left(\frac{z(8z-3)}{1-z}\ln z+2z+z^2\right),
$$

$$
2\varepsilon^2\int\frac{d\Omega_k}{2\pi}T_{22} = \rho\left(\frac{4z}{(1-z)^2}L_0-\frac{8}{(1-z)^2}\right)+\frac{16}{(1-z)^2}\ln z L_Q-
$$

$$
-\frac{2z(1+2(1-z)^2)}{(1-z)^4}(A\ln z+B)-A\frac{3z-1}{z(1-z)^3}+ \tag{F.1}
$$

$$
+\frac{2L_0}{z(1-z)^3}\left(\frac{1+4z(z^2+z-1)}{1-z}\ln z+z^3-z^2+4z-1\right),
$$

$$
2\varepsilon^2\int\frac{d\Omega_k}{2\pi}T_{21} = \frac{2z^2}{(1-z)^4}(A\ln z+B)+\frac{3z-1}{(1-z)^3}A+
$$

$$
+\frac{2L_0}{(1-z)^3}\left(\frac{-1+4z-4z^2-4z^3}{1-z}\ln z-2z^2-2z+1\right),
$$

$$
2\varepsilon^2\int\frac{d\Omega_k}{2\pi}T_{12} = \frac{2z(2-z)}{(1-z)^4}(A\ln z+B)+\frac{3-z}{(1-z)^3}A+
$$

$$
+\frac{2L_0}{(1-z)^3}\left(\frac{3-8z}{1-z}\ln z-1-2z\right),
$$

where ρ, A, and B are given by Eq. (1.2.13). It is remarkable to see that the relation

$$
\int\frac{d\Omega_k}{2\pi}\left[4zT_g+Q_l^2(T_{11}+z^2T_{22}+zT_{12}+zT_{21})\right]=0 \tag{F.2}
$$

is fulfilled, leading to the factorization of the virtual corrections in Eq. (1.2.13).

APPENDIX G

To perform the angular integration in (1.2.23) we first represent the integrand in the form

$$\frac{\varepsilon^2 \alpha^2 (Q_{sc}^2) I^\gamma}{Q_{sc}^4} = \frac{F(t_1, t_2)}{t_1 t_2}, \tag{G.1}$$

where $t_{1,2} = (1 - c_{1,2})/2$, $c_{1,2} = \cos \theta_{1,2}$, and $\theta_{1,2}$ are the angles between nontagged photon momentum k_2 and the momenta of the initial and the scattered electrons. Note that $F(t_1, t_2)$ behaves regularly for $t_1 \to 0$ or $t_2 \to 0$. This can be easily seen by considering the limiting cases for the quantity I^γ.

For the case $t \to 0$, which corresponds to the second photon being emitted close to the direction of the incoming electron, one obtains from Eq. (1.2.24)

$$I^\gamma|_{t \to 0} = \frac{Q^2}{x_2 t}(z^2 + (z - x_2)^2)\left[x_t F_2(x_t, Q_t^2) \times \right.$$

$$\left. \times \left(\frac{M^2}{Q_t^2} - \frac{1 - y}{x^2 y^2 (z - x_2)} \right) - F_1(x_t, Q_t^2) \right], \tag{G.2}$$

while for the case $s \to 0$, corresponding to the second photon being almost collinear to the final electron,

$$I^\gamma|_{s \to 0} = -\frac{Q^2 z}{y_2 s}(1 + (1 + y_2)^2)\left[x_b F_2(x_b, Q_b^2) \times \right.$$

$$\left. \times \left(\frac{M^2}{Q_b^2} - \frac{1 - y}{x^2 y^2 z (1 + y_2)} \right) - F_1(x_b, Q_b^2) \right], \tag{G.3}$$

see Eqs.(1.2.20) and (1.2.27) for the notation. The r.h.s. of Eq. (G.1) is easily seen to be

$$\frac{\varepsilon^2 \alpha^2 (Q_{sc}^2) I^\gamma}{Q_{sc}^4}\bigg|_{t \to 0} = \frac{1}{t_1 t_2} \frac{a}{16\pi x_2^2} \frac{z^2 + (z - x_2)^2}{z(z - x_2)} \Sigma(x_t, y_t, Q_t^2), \quad (G.4)$$

$$\frac{\varepsilon^2 \alpha^2 (Q_{sc}^2) I^\gamma}{Q_{sc}^4}\bigg|_{s \to 0} = \frac{1}{t_1 t_2} \frac{a}{16\pi x_2^2} \frac{1 + (1 + y_2)^2}{1 + y_2} \Sigma(x_b, y_b, Q_b^2), \quad (G.5)$$

where $a = (1 - \cos \theta)/2$.

For the phase space of the photon we use the following representation:

$$\int \frac{d^3 k_2}{\omega_2} = \varepsilon^2 \int x_2 \, dx_2 \, d\Omega_2 = 4\varepsilon^2 \int x_2 \, dx_2 \int \frac{dt_1 \, dt_2}{\sqrt{D}} \Theta(D),$$

$$D = (t_2 - y_-)(y_+ - t_2), \quad y_\pm = t_1(1 - 2a) + a \pm 2\sqrt{a(1-a)t_1(1-t_1)}. \tag{G.6}$$

The region of integration is determined by the conditions

$$\sigma_1 < t_1 < 1, \quad \sigma_2 < t_2 < 1, \quad D > 0, \quad \sigma_1 = \frac{\theta_0^2}{4}, \quad \sigma_2 = \frac{\theta_0'^2}{4}. \tag{G.7}$$

Using the substitution

$$t_2 \to t_2(t_1, u) = \frac{(a - t_1)^2(1 + u^2)}{y_+ + u^2 y_-}, \tag{G.8}$$

and the identity

$$\int\limits_{\sigma_1}^{1} dt_1 \int\limits_{\sigma_2}^{1} dt_2 \frac{F(t_1, t_2)}{t_1 t_2 \sqrt{D}} \Theta(D) = \frac{\pi}{a} \left[F(a, 0) \ln \frac{a}{\sigma_2} + F(0, a) \ln \frac{a}{\sigma_1} \right] +$$

$$+ 2 \int\limits_{0}^{\infty} \frac{du}{1 + u^2} \lim\limits_{\eta \to 0} \left[\int\limits_{\eta}^{1} \frac{dt_1}{t_1 |t_1 - a|} (F(t_1, t_2) - F(a, 0)) + \right.$$

$$\left. + \int\limits_{\eta}^{a} \frac{dt_1}{t_1 a} (F(a, 0) - F(0, a)) \right], \tag{G.9}$$

which is valid for $\sigma_1, \sigma_2 \ll a$, we obtain for Z from Eq. (1.2.25) the following expression:

$$Z = -\frac{4(1-c)}{zQ^2} \int\limits_{0}^{\infty} \frac{du}{1 + u^2} \lim\limits_{\eta \to 0} \left[\int\limits_{\eta}^{1} \frac{dt_1}{t_1 |t_1 - a|} \times \right.$$

$$\left. \times \int\limits_{0}^{x_m} \frac{dx_2}{x_2} (\Phi(t_1, t_2(t_1, u)) - \Phi(a, 0)) + \int\limits_{\eta}^{a} \frac{dt_1}{t_1 a} \int\limits_{0}^{x_m} \frac{dx_2}{x_2} (\Phi(a, 0) - \Phi(0, a)) \right], \tag{G.10}$$

where

$$\Phi(t_1, t_2) = \left. \frac{\alpha^2(Q_{sc}^2)stI^\gamma}{Q_{sc}^4}\right|_{c_1=1-2t_1,\ c_2=1-2t_2(t_1,u),\ c=1-2a} . \quad \text{(G.11)}$$

The upper limit of the x_2-integration, x_m, may be deduced from [42]. It has the form

$$x_m = \frac{z(e+p) - \Delta_m - Y(e+z) - (p-z)Yc}{z+e-Y+(p-z)c_1+Yc_2}, \qquad e = \frac{E_p}{\varepsilon},$$

$$p = \frac{P_p}{\varepsilon}, \qquad \Delta_m = \frac{(M+m_\pi)^2 - M^2}{2\varepsilon^2}. \quad \text{(G.12)}$$

This finally leads to Eq. (1.2.25).

It is important to note that while calculating Z one encounters neither collinear nor infrared singularities.

REFERENCES

1. **Sloan T., Voss R., Smadja G.** — Phys. Rep., 1988, v.162, p.45.

2. **Ashman J. for EMC Coll.** — Nucl. Phys., 1989, v.B328, p.1.

3. **Anselmino M., Efremov A., Leader E.** — Phys. Rep., 1995, v.261, p.1.

4. **Mo L., Tsai Y.** — Rev. Mod. Phys., 1969, v.41, p.205.

5. **Bardin D.Y., Shumeiko N.M.** — Nucl. Phys., 1977, v.B127, p.242.

6. **Akhundov A., Bardin D., Kalinovskaya L. et al.** — Fortsch. Phys., 1996, v.44, p.373.

7. **Kuzhir P.P., Shumeiko N.M.** — Sov. J. Nucl. Phys., 1992, v.55, p.1086.

8. **Badelek B., Bardin D., Kurek K. et al.** — Z. Phys., 1995, v.C66, p.591.

9. **Akushevich I., Bottcher H., Ryckbosch D.** — In: Proc. of Hamburg Int. Conf. on Monte Carlo Generators for HERA Physics, 1998/99, p.554–565; hep-ph/9906408.

10. **Akhundov A.A., Bardin D.Y., Shumeiko N.M.** — Sov. J. Nucl. Phys., 1977, v.26, p.660.

11. **Kukhto T.V., Shumeiko N.M.** — Nucl. Phys., 1983, v.B219, p.412.

12. **Akushevich I.V., Shumeiko N.M.** — J. Phys., 1994, v.G20, p.513.

13. **Kuraev E.A., Merenkov N.P., Fadin V.S.** — YaF, 1988, v.47, p.1593.

14. **Bohm M., Spiesberger H.** — Nucl. Phys., 1987, v.B294, p.1081.

15. **Bardin D.Y., Burdik C., Khristova P.C. et al.** — Z. Phys., 1989, v.C42, p.679.

16. **Akushevich I.V., Ilichev A.N., Shumeiko N.M.** — Phys. Atom. Nucl., 1998, v.61, p.2154.

17. **Akushevich I.V., Ilichev A.N., Shumeiko N.M.** — J. Phys., 1998, v.G24, p.1995.

18. **Soroko A.V., Shumeiko N.M.** — Sov. J. Nucl. Phys., 1989, v.49, p.838.

19. **Akushevich I.** — Eur. Phys. J., 1999, v.C8, p.457.

20. **Akushevich I., Kuzhir P.** — Phys. Lett., 2000, v.B474, p.411.

21. **Akushevich I., Shumeiko N., Soroko A.** — Eur. Phys. J., 1999, v.C10, p.681.

22. **Maximon L.C., Parke W.C.** — Phys. Rev., 2000, v.C61, p.045502.

23. **Maximon L.C., Tjon J.A.** — nucl-th/0002058.

24. **Templon J.A., Vellidis C.E., Florizone R.E. et al.** — Phys. Rev., 2000, v.C61, p.014607.

25. FERRAD 3.5. This code was firstly created by J.Dress for EMC and further developed by M.Dueren.

26. **Magnussen N. et al.** — In: Proc. of Hamburg Workshop on Physics at HERA, Buchmüller W., Ingelman G. (eds.), 1991, v.3.

27. **Kwiatkowski A., Spiesberger H., Mohring H.J.** — Comp. Phys. Commun., 1992, v.69, p.155.

28. **Arbuzov A., Bardin D., Bluemlein J. et al.** — Comp. Phys. Commun., 1996, v.94, p.128.

29. **Akushevich I., Ilichev A., Shumeiko N. et al.** — Comp. Phys. Commun., 1997, v.104, p.201.

30. **Akushevich I., Nagaitsev A.** — J. Phys., 1998, v.G24, p.2235.

31. **Kuraev E.A., Fadin V.S.** — Sov. J. Nucl. Phys., 1985, v.41, p.466.

32. **Skrzypek M.** — Acta Phys. Polonica, 1992, v.B23, p.135.

33. **Kuraev E.A., Merenkov N.P., Fadin V.S.** — YaF, 1987, v.45, p.782.

34. **Akhundov A.A., Bardin D.Y., Shumeiko N.M.** — Sov. J. Nucl. Phys., 1986, v.44, p.988.

35. **Akushevich I.V., Kukhto T.V., Pacheco F.** — J. Phys., 1992, v.G18, p.1737.

36. **Favart L., Gruwe M., Marage P. et al.** — Z. Phys., 1996, v.C72, p.425.

37. **Berends F.A. et al.** — Phys. Lett., 1981, v.B103, p.124;
    Berends F.A. et al. — Nucl. Phys., 1982, v.B206, p.61.

38. **Arbuzov A.B., Kuraev E.A., Merenkov N.P. et al.** — Nucl. Phys., 1996, v.B474, p.271.

39. **Spiesberger H. et al.** — In: Proc. of Hamburg Workshop on Physics at HERA, Buchmüller W., Ingelman G., (eds.), 1991, v.3.

40. **Jadach S., Jezabek M., Placzek W.** — Phys. Lett., 1990, v.B248, p.417.

41. **Krasny M.W., Placzek W., Spiesberger H.** — Z. Phys., 1992, v.C53, p.687.

42. **Bardin D., Kalinovskaya L., Riemann T.** — Z. Phys., 1997, v.C76, p.487.

43. **Ahmed T. et al.** — Z. Phys., 1995, v.C66, p.529.

44. **Klein M. for H1 Coll.** — In: Proc. of ICHEP'98 Conference, Vancouver, 1998, contributed paper no. 535.

45. **Arbuzov A.B. et al.** — Nucl. Phys., 1997, v.B485, p.457;
    Merenkov N.P. et al. — Acta Phys. Polonica, 1997, v.B28, p.491.

46. **Kuraev E.A., Merenkov N.P., Fadin V.S.** — Sov. J. Nucl. Phys., 1987, v.45, p.486.

47. **Feynman R.P.** — Photon-Hadron Interactions. W.A. Benjamin, Inc., Reading, Massachusetts, 1972.

48. **Merenkov N.P.** — Sov. J. Nucl. Phys., 1988, v.48, p.1073.

49. **Baier V.N., Fadin V.S., Khoze V.A.** — Nucl. Phys., 1973, v.B65, p.381.

50. **Kinoshita T.** — J. Math. Phys. (N.Y.), 1962, v.3, p.650;
    Lee T.D., Nauenberg M. — Phys. Rev., 1964, v.133, p.1549.

51. **Anlauf H., Arbuzov A.B., Kuraev E.A. et al.** — JETP Lett., 1997, v.66, p.391; Erratum ibid.,
    1998, v.67, p.305.

52. **Anlauf H., Arbuzov A., Kuraev E. et al.** — JHEP, 1998, v.9810, p.013.

53. **Akushevich I., Arbuzov A., Kuraev E.** — Phys. Lett., 1998, v.B432, p.222.

54. **Kleiss R.** — Z. Phys., 1987, v.C33, p.433.

55. **Adams D. et al.** — Phys. Rev., 1997, v.D56, p.5330.

56. **Ackerstaff K. et al.** — Phys. Lett., 1997, v.B404, p.383.

57. **Barbieri R., Mignaco J.A., Remiddi E.** — IL Nuovo Cim., 1972, v.A11, p.824.

58. **Gagunashvili N.D.** — Nucl. Instr. and Meth., 1994, v.A343, p.606;
    Gagunashvili N.D. et al. — JINR Preprint E1–96–483, Dubna, 1996.

59. **Bluemlein J., Levman G., Spiesberger H.** — J. Phys., 1993, v.G19, p.1695.

60. **Arbuzov A.B., Kuraev E.A., Merenkov N.P. et al.** — YaF, 1996, v.59, p.878.

61. **Konchatnij M.I., Merenkov N.P.** — Pisma v ZhETF, 1999, v.69, p.645.

62. **Arbuzov A., Kuraev E., Merenkov N. et al.** — JHEP, 1998, v.9812, p.009.

63. **Aid S. et al.** — Nucl. Phys., 1996, v.B470, p.3.

64. **Baier V.N., Khoze V.A.** — ZhETF, 1965, v.48, p.946; YaF, 1965, v.2, p.287.

65. **Brown D.H., Worstell W.A.** — Phys. Rev., 1996, v.D54, p.3237;
    Eidelman S. et al. — Z. Phys., 1995, v.C67, p.585;
    Jegerlehner F. — In: Proc. of Karlsrue Workshop on Hadron Production Cross Sections at
    DAΦNE, Hagel U.V. et al. (eds.), 1996, v.1, p.81.

66. **Anlauf H., Arbuzov A., Kuraev E.A. et al.** — Phys. Rev., 1999, v.D59, p.014003.

67. **Arbuzov A.B. et al.** — Nucl. Phys., 1997, v.B483, p.83.

68. **Jadach S., Skrzypek M., Ward B.F.L.** — Phys. Rev., 1993, v.D47, p.3733.

69. **Nicrosini O., Trentadue L.** — Phys. Lett., 1987, v.B196, p.551.

70. **Catani S., Trentadue L.** — JETP Lett., 1990, v.51, p.83.

71. **Lipatov L.N.** — YaF, 1974, v.20, p.181;
    Altarelli G., Parisi G. — Nucl. Phys., 1977, v.B126, p.298.

72. **Spagnolo S.** — KLOE memo No.139, 1998.

73. **Kuraev E.A., Schiller A., Serbo V.G. et al.** — Nucl. Phys., 2000, v.B570, p.359.